EUROPEAN ORGANIZATION FOR NUCLEAR RESEARCH (CERN)

FERMILAB-PUB-16-253-CMS

CERN-EP/2016-139
2016/07/05

CMS-TOP-12-042

Measurement of the differential cross sections for top quark pair production as a function of kinematic event variables in pp collisions at $\sqrt{s} = 7$ and 8 TeV

The CMS Collaboration*

arXiv:1607.00837v1 [hep-ex] 4 Jul 2016

Abstract

Measurements are reported of the normalized differential cross sections for top quark pair production with respect to four kinematic event variables: the missing transverse energy; the scalar sum of the jet transverse momentum (p_{T}); the scalar sum of the p_{T} of all objects in the event; and the p_{T} of leptonically decaying W bosons from top quark decays. The data sample, collected using the CMS detector at the LHC, consists of 5.0 fb^{-1} of proton-proton collisions at $\sqrt{s} = 7$ TeV and 19.7 fb^{-1} at $\sqrt{s} = 8$ TeV. Top quark pair events containing one electron or muon are selected. The results are presented after correcting for detector effects to allow direct comparison with theoretical predictions. No significant deviations from the predictions of several standard model event simulation generators are observed.

Submitted to Physical Review D

© 2016 CERN for the benefit of the CMS Collaboration. CC-BY-3.0 license

*See Appendix B for the list of collaboration members

1 Introduction

The CERN LHC produced millions of top quark pairs ($t\bar{t}$) in 2011 and 2012. This allows for a detailed investigation of the kinematic event properties of $t\bar{t}$ production such as the missing transverse energy (E_T^{miss}), the scalar sum of the jet transverse momenta (H_T), the scalar sum of the transverse momenta of all objects (S_T), and the transverse momentum (p_T^W) of leptonically decaying W bosons produced in top quark decays. These measurements can be used to verify current theoretical models, along with their implementation in simulations of $t\bar{t}$ production, and also to measure rare standard model (SM) processes such as $t\bar{t}$ production in association with a W, Z, or Higgs boson. Since top quark pair production is a major background for many searches for physics beyond the SM, it is important that the properties of $t\bar{t}$ events are well understood.

Here, we report measurements carried out using the CMS detector [1] at the LHC at two different proton–proton center-of-mass energies. The data samples used include integrated luminosities of 5.0 fb^{-1} collected in 2011 at $\sqrt{s} = 7$ TeV and 19.7 fb^{-1} from 2012 at $\sqrt{s} = 8$ TeV. The $t\bar{t}$ production cross section is measured as a function of E_T^{miss}, H_T, S_T, and p_T^W, corrected for detector effects, and compared with the predictions from different event generators. Differential $t\bar{t}$ cross sections have previously been measured at the Tevatron [2, 3], and at the LHC [4–9]. These previous measurements study the $t\bar{t}$ production cross section as a function of the top quark kinematics and the kinematics of the $t\bar{t}$ system. The results presented here are complementary, since the $t\bar{t}$ production cross section is measured as a function of variables that do not require the reconstruction of the top quarks from their decay products.

Top quarks decay with close to 100% probability into a W boson and a bottom quark. In this article, we consider the channel in which one of the W bosons decays leptonically into a charged lepton (electron or muon) along with its associated neutrino, while the other W boson decays hadronically. This channel has a branching fraction of around 15% for direct decay to each lepton flavor and a relatively clean experimental signature, including an isolated, high-transverse-momentum lepton, large E_T^{miss} from the undetected neutrino, and multiple hadronic jets. Two jets are expected to contain b hadrons from the hadronization of the b quarks produced directly in the $t \to bW$ decay, while other jets (from the hadronic W boson decay or gluon radiation) will typically contain only light-quark flavors.

2 The CMS detector

The central feature of the CMS apparatus is a superconducting solenoid of 6 m internal diameter, providing a magnetic field of 3.8 T. Within the solenoid volume are a silicon pixel and strip tracker, a lead tungstate crystal electromagnetic calorimeter, and a brass and scintillator hadron calorimeter, each composed of a barrel and two endcap sections. Muons are measured in gas-ionisation detectors embedded in the steel flux-return yoke outside the solenoid. Extensive forward calorimetry complements the coverage provided by the barrel and endcap detectors.

A more detailed description of the CMS detector, together with a definition of the coordinate system used and the relevant kinematic variables, can be found in Ref. [1].

3 Simulation

For the Monte Carlo (MC) simulation of the $t\bar{t}$ signal sample the leading-order MADGRAPH v5.1.5.11 event generator [10] is used with relevant matrix elements for up to three addi-

tional partons implemented. Theoretical production cross section values of $177.3\,^{+4.6}_{-6.0}$ (scale) $\pm$ 9.0 (PDF+α_S) pb at $\sqrt{s} = 7$ TeV, and $252.9\,^{+6.4}_{-8.6}$ (scale) $\pm$ 11.7 (PDF+α_S) pb at $\sqrt{s} = 8$ TeV, are used for the normalization of these samples. These cross sections are calculated with the Top++2.0 program to next-to-next-to-leading order (NNLO) in perturbative QCD, including soft-gluon resummation to next-to-next-to-leading-logarithm (NNLL) order [11], and assuming a top quark mass $m_t = 172.5$ GeV. The first uncertainty comes from the independent variation of the renormalization (μ_R) and factorization (μ_F) scales, while the second one is associated with variations in the parton distribution function (PDF) and α_S, following the PDF4LHC prescription with the MSTW2008 68% CL NNLO, CT10 NNLO, and NNPDF2.3 5f FFN PDF sets [12–16].

The generated events are subsequently processed with PYTHIA v6.426 [17] for parton showering and hadronization. The PYTHIA parton shower is matched to the jets from the hard quantum chromodynamics (QCD) matrix element via the MLM prescription [18] with a transverse momentum (p_T) threshold of 20 GeV. The CMS detector response is simulated using GEANT4 [19].

Independent $t\bar{t}$ samples are also generated at both $\sqrt{s} = 7$ TeV and $\sqrt{s} = 8$ TeV with POWHEG v2 r2819 [20–22]. At 8 TeV, additional samples are generated with both MC@NLO v3.41 [23] and POWHEG v1.0 r1380 [20–22]. All of the POWHEG samples are interfaced with both PYTHIA and HERWIG v6.520 [24], whereas the MC@NLO generator is interfaced with HERWIG for parton showering. These samples, which are all generated to next-to-leading order accuracy, are used for comparison with the final results.

The most significant backgrounds to $t\bar{t}$ production are events in which a W boson is produced in association with additional jets. Other backgrounds include single top quark production, Z boson production in association with multiple jets, and QCD multijet events where hadronic activity is misidentified as a lepton. The simulation of background from W and Z boson production in association with jets is also performed using the combination of MADGRAPH and PYTHIA, with a p_T matching threshold of 10 GeV in this case. These samples are referred to as W+jets and Z+jets, respectively. Single top quark production via t- and s-channel W boson exchange [25] and with an associated on-shell W boson [26] are generated using POWHEG. The QCD multijet processes are simulated using PYTHIA. The event yields of the background processes are normalized according to their predicted production cross section values. These are from NNLO calculations for W+jets and Z+jets events [27, 28], next-to-leading order calculations with NNLL corrections for single top quark events [29], and leading-order calculations for QCD multijet events [17].

Samples are generated using the CTEQ6L PDFs [30] for MADGRAPH samples, the CT10 PDFs [31] for POWHEG samples, and the CTEQ6M PDFs [30] for MC@NLO. The PYTHIA Z2 tune is used to describe the underlying event in both the MADGRAPH and POWHEG + PYTHIA samples at $\sqrt{s} = 7$ TeV, whereas the Z2* tune is used for the corresponding samples at $\sqrt{s} = 8$ TeV [32]. The underlying event in the POWHEG + HERWIG samples is described by the AUET2 tune [33], whereas the default tune is used in the MC@NLO + HERWIG sample.

The value of the top quark mass is fixed to $m_t = 172.5$ GeV in all samples. In all cases, PYTHIA is used for simulating the gluon radiation and fragmentation, following the prescriptions of Ref. [34]. Additional simulated hadronic pp interactions ("pileup"), in the same or nearby beam crossings, are overlaid on each simulated event to match the high-luminosity conditions in actual data taking.

Previous measurements of differential $t\bar{t}$ production cross sections at the LHC [4, 5, 8] showed

that several of the $t\bar{t}$ event generators considered in this analysis predict a harder top quark p_T spectrum than that observed in data. An additional simulated $t\bar{t}$ sample is considered here, where the sample produced with the MADGRAPH event generator is reweighted to improve the agreement of the top quark p_T spectrum with data.

4 Event reconstruction and selection

Parallel selection paths for the two lepton types are implemented, resulting in samples classified as electron+jets and muon+jets. The trigger for the electron+jets channel during the $\sqrt{s} = 7$ TeV data taking selects events containing an electron candidate with $p_T > 25$ GeV and at least three reconstructed hadronic jets with $p_T > 30$ GeV. In the $\sqrt{s} = 8$ TeV data, at least one electron candidate with $p_T > 27$ GeV is required, with no additional requirement for jets. In the muon+jets channel, at least one isolated muon candidate with $p_T > 24$ GeV is required at the trigger level. Each candidate event is required to contain at least one well-measured vertex [35], located within the pp luminous region in the center of CMS.

Events are reconstructed using a particle-flow (PF) technique [36, 37], which combines information from all subdetectors to optimize the reconstruction and identification of individual long-lived particles.

Electron candidates are selected with a multivariate technique using calorimetry and tracking information [38]. Inputs to the discriminant include information about the calorimeter shower shape, track quality, track-shower matching, and a possible photon conversion veto. Electron candidates are required to have $E_T > 30$ GeV and pseudorapidity in the range $|\eta| < 2.5$. The low-efficiency region $1.44 < |\eta| < 1.57$ between the barrel and endcap sections of the detector is excluded. Muon candidates are selected with tight requirements on track and vertex quality, and on hit multiplicity in the tracker and muon detectors [39]. These requirements suppress cosmic rays, misidentified muons, and nonprompt muons from decay of hadrons in flight. Muon candidates are required to have $p_T > 26$ GeV and $|\eta| < 2.1$.

For the lepton isolation requirement, a cone of size $\Delta R = \sqrt{(\Delta\eta)^2 + (\Delta\phi)^2}$ is constructed around the lepton direction, where $\Delta\eta$ and $\Delta\phi$ are the differences in pseudorapidity and azimuthal angle (in radians), respectively, between the directions of the lepton and another particle. The p_T values of charged and neutral particles found in this cone are summed, excluding the lepton itself and correcting for the effects of pileup [38]. The relative isolation variable $I(\Delta R)$ is defined as the ratio of this sum to the lepton p_T. Lepton candidates are selected if they satisfy $I(0.3) < 0.1$ for electrons, and $I(0.4) < 0.12$ for muons.

Reconstructed particles are clustered into jets using the anti-k_T algorithm [40] with a distance parameter of 0.5. The measured p_T of each jet is corrected [41] for known variations in the jet energy response as a function of the measured jet η and p_T. The jet energy is also corrected for the extra energy deposition from pileup interactions [42, 43]. Jets are required to pass loose identification requirements to remove calorimeter noise [44]. Any such jet whose direction is less than $\Delta R = 0.3$ from the identified lepton direction is removed. For the identification of b quark jets ("b tagging"), a "combined secondary vertex" algorithm [45] is used, taking into account the reconstructed secondary vertices and track-based lifetime information. The b tagging threshold is chosen to give an acceptance of 1% for light-quark and gluon jets with a tagging efficiency of 65% for b quark jets.

The final selection requires exactly one high-p_T, isolated electron or muon. Events are vetoed if they contain an additional lepton candidate satisfying either of the following criteria: an

electron with $p_T > 20\,\text{GeV}$, $|\eta| < 2.5$, and $I(0.3) < 0.15$; or a muon, with looser requirements on hit multiplicity, and with $p_T > 10\,\text{GeV}$, $|\eta| < 2.5$, and $I(0.4) < 0.2$. The event must have at least four jets with $p_T > 30\,\text{GeV}$, of which at least two are tagged as containing b hadrons.

After the final selection, 26 290 data events are found at $\sqrt{s} = 7\,\text{TeV}$, and 153 223 at $\sqrt{s} = 8\,\text{TeV}$. The $t\bar{t}$ contribution to these event samples, as estimated from simulation, is about 92%. The fraction of true signal events in the samples is 78%. Misidentified all-hadronic or dileptonic $t\bar{t}$ events, and events containing tau leptons among the $t\bar{t}$ decay products, comprise 14% of the samples. The remaining events are approximately 4% single top quark events, 2% W/Z+jets events, and 2% QCD multijet events. The efficiency for signal events to satisfy the final selection criteria is about 8%, as determined from simulation.

5 Cross section measurements

We study the normalized $t\bar{t}$ differential production cross section as a function of four kinematic event variables: E_T^{miss}, H_T, S_T, and p_T^W.

The variable E_T^{miss} is the magnitude of the missing transverse momentum vector $\vec{p}_T^{miss}$, which is defined as the projection on the plane perpendicular to the beams of the negative vector sum of the momenta of all PF candidates in the event:

$$E_T^{miss} = \left[\left(-\sum_i p_x^i \right)^2 + \left(-\sum_i p_y^i \right)^2 \right]^{\frac{1}{2}},$$

where p_x^i and p_y^i are the x and y momentum components of the ith candidate, and the sums extend over all PF candidates. The measured E_T^{miss} is corrected for pileup and nonuniformities in response as a function of ϕ [46].

The variable H_T is defined as the scalar sum of the transverse momenta of all jets in the event,

$$H_T = \sum_{\text{all jets}} p_T^{jet},$$

where the sum extends over all jets having $p_T > 20\,\text{GeV}$ and $|\eta| < 2.5$.

The variable S_T is the scalar sum of H_T, E_T^{miss}, and the p_T of the identified lepton,

$$S_T = H_T + E_T^{miss} + p_T^{lepton}.$$

Finally, p_T^W is the magnitude of the transverse momentum of the leptonically decaying W boson, which is derived from the momentum of the isolated lepton and $\vec{p}_T^{miss}$

$$p_T^W = \sqrt{\left(p_x^{lepton} + p_x^{miss}\right)^2 + \left(p_y^{lepton} + p_y^{miss}\right)^2},$$

where p_x^{lepton} and p_y^{lepton} are the transverse components of $\vec{p}^{lepton}$, and p_x^{miss} and p_y^{miss} are the transverse components of $\vec{p}_T^{miss}$.

Figures 1 and 2 show the observed distributions of E_T^{miss}, H_T, S_T, and p_T^W, in the $\sqrt{s} = 8\,\text{TeV}$ data samples, compared to the sum of the corresponding signal and background distributions from simulation.

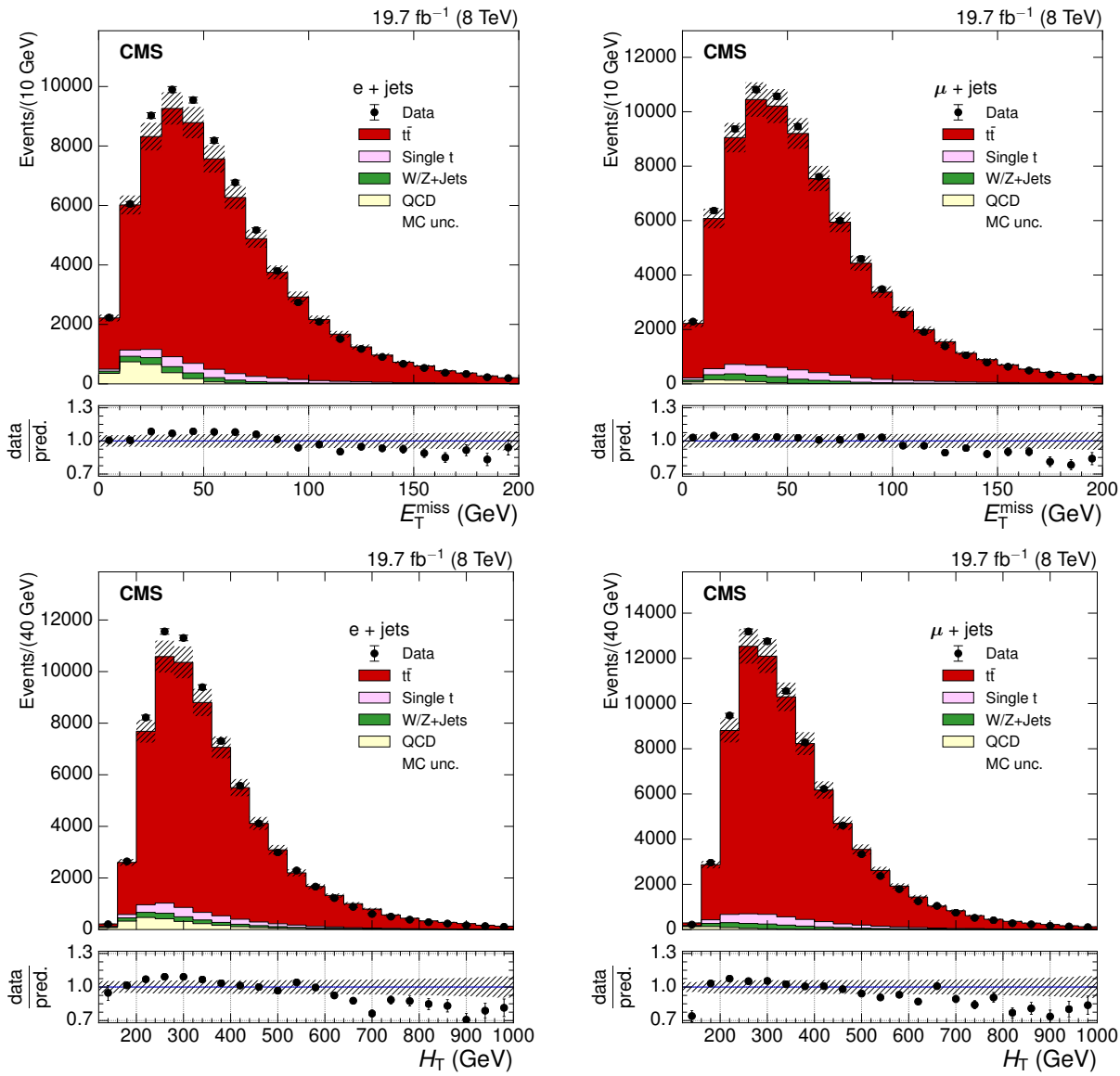

Figure 1: The observed distributions of E_T^{miss} (top) and H_T (bottom) in the $\sqrt{s} = 8$ TeV electron+jets (left) and muon+jets (right) data samples, compared to predictions from simulation. The points are the data histograms, with the vertical bars showing the statistical uncertainty, and the predictions from the simulation are the solid histograms. The shaded region shows the uncertainty in the values from simulation. These include contributions from the statistical uncertainty and the uncertainty in the $t\bar{t}$ cross section. The lower plots show the ratio of the number of events from data and the prediction from the MC simulation.

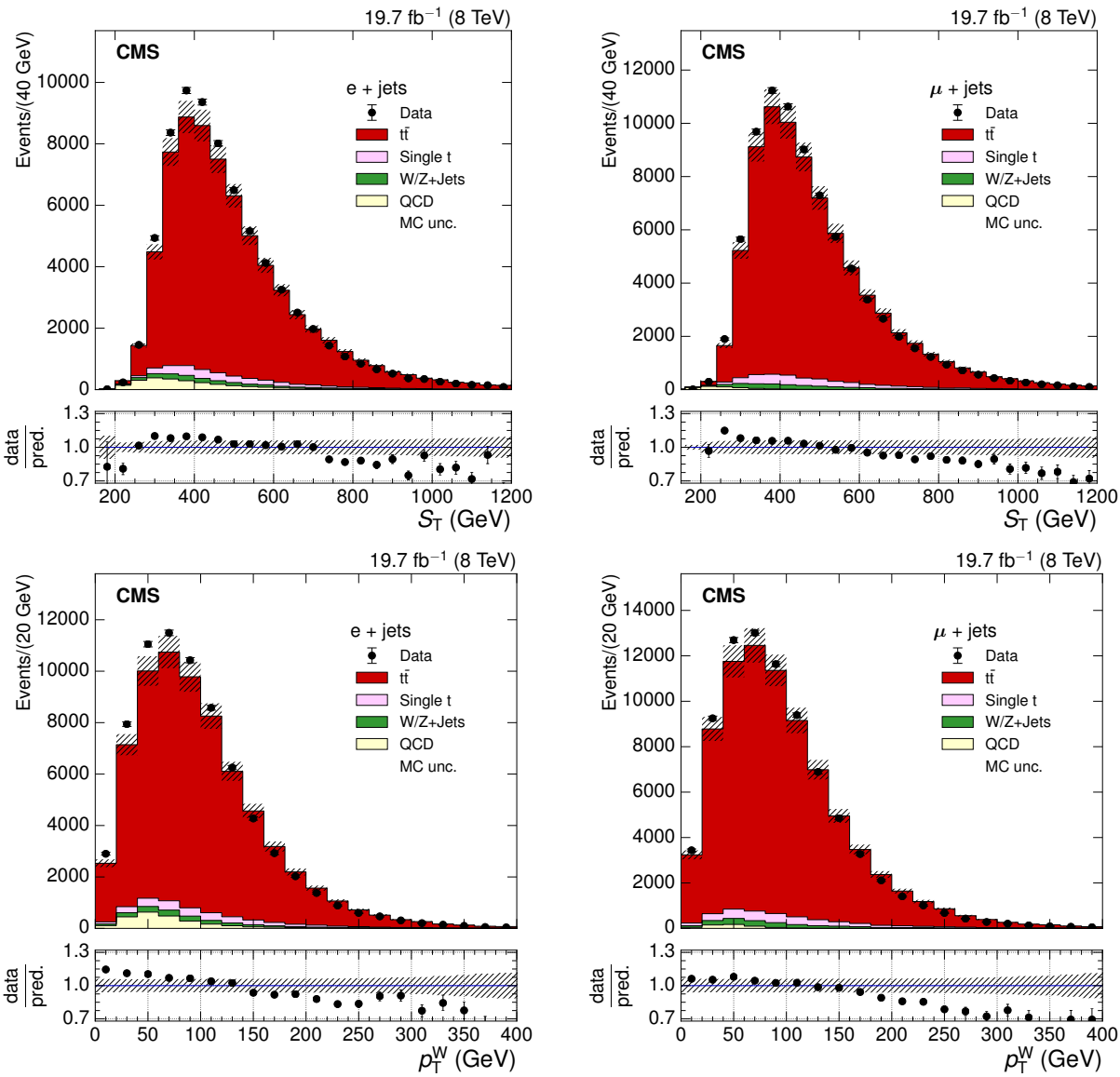

Figure 2: The observed distributions of S_T (top) and p_T^W (bottom) in the $\sqrt{s} = 8$ TeV electron+jets (left) and muon+jets (right) data samples, compared to predictions from simulation. The points are the data histograms, with the vertical bars showing the statistical uncertainty, and the predictions from the simulation are the solid histograms. The shaded region shows the uncertainty in the values from simulation. These include contributions from the statistical uncertainty and the uncertainty in the $t\bar{t}$ cross section. The lower plots show the ratio of the number of events from data and the prediction from the MC simulation.

For simulated $t\bar{t}$ signal events, these four kinematic variables are also calculated using the momenta of particles in the event, before the simulation of the detector response. We refer to the quantities calculated in this way as the generated variables. The generated value of E_T^{miss} is the magnitude of the vector sum of the p_T of all neutrinos in the event. The long-lived particles in the event are clustered into jets in the same way as the reconstructed particles. The generated value of H_T is the sum of the magnitudes of the p_T of these jets with $p_T > 20\,\text{GeV}$ and $|\eta| < 2.5$. The generated values of S_T and p_T^W are calculated in the same way as the corresponding reconstructed variables, using the $\vec{p}_T$ of the charged lepton from the leptonic decay of a W boson coming from $t \to bW$ decay.

The choice of bin widths for this measurement is optimized separately for each kinematic event variable to minimize the migration between bins. This optimization is based on three criteria: (i) of the simulated signal events for which the value of the generated variable falls in the bin, at least 50% are required to have the reconstructed variable in the same bin (this is sensitive to migration of events out of the bin); (ii) of the simulated signal events for which the value of the reconstructed variable falls in the bin, at least 50% are required to have the generated variable in the same bin (this is sensitive to migration of events into the bin); (iii) the number of reconstructed simulation events in a bin is required to be more than 100. These criteria ensure that bin-to-bin migrations are kept small, while allowing a differential cross section measurement with reasonable granularity.

The number of $t\bar{t}$ events in each bin of each kinematic event variable, and in each channel, is obtained by subtracting the expected contributions of background processes from data. The contributions of single top quark, and W or Z boson plus jet events are estimated from simulation.

In the case of the QCD multijet background, the contribution is estimated from data using a control region where the selection criteria are modified to enrich the contribution of QCD multijet events. In the electron+jets channel, the control region is obtained by inverting the photon conversion veto on the electron. In addition to this, the number of b-tagged jets is required to be exactly zero. The small contamination of $t\bar{t}$, single top, W+jets, and Z+jets events in this control region, as estimated from simulation, is subtracted from the data. Then, the ratio of simulated QCD multijet events in the control region and the signal region is used to scale the normalization of the data-driven QCD multijet estimate from the control region to the signal region in the data. The control region in the muon+jets channel is obtained by inverting the isolation criterion on the muon in the selected events, and by requiring exactly zero b-tagged jets. The jet selection criterion is also modified, requiring at least three jets. The same procedure is then followed to estimate the contribution of QCD mulitjet events in the muon+jets signal region.

The number of $t\bar{t}$ events from data in each bin is then corrected for the small fractions of dileptonic, all-hadronic, and tau $t\bar{t}$ events in the final sample, as determined from simulation, and for experimental effects, such as detector resolution, acceptance, and efficiency. This correction is performed by constructing a response matrix that maps the generated values to the reconstructed values for the four kinematic variables in the simulated $t\bar{t}$ signal events. The response matrix is constructed using the MADGRAPH $t\bar{t}$ sample. This matrix is then inverted, using regularized singular-value decomposition [47] in the ROOUNFOLD [48] software framework. Since we impose no requirements on the generated events, the procedure corrects to the full signal phase space.

The fully-corrected numbers of $t\bar{t}$ events in the electron+jets and muon+jets channels yield consistent results. These are then added and used to calculate the normalized $t\bar{t}$ differential

production cross section with respect to each kinematic event variable, X, using:

$$\frac{1}{\sigma}\frac{\mathrm{d}\sigma_j}{\mathrm{d}X} = \frac{1}{N}\frac{x_j}{\Delta_j^X}\,, \tag{1}$$

where x_j represents the number of unfolded signal events in bin j, Δ_j^X is the width of bin j; σ is the total $\mathrm{t\bar{t}}$ production cross section, and $N = \sum_i x_i$ is the total number of unfolded signal events.

6 Systematic uncertainties

The systematic uncertainties in the experimental and theoretical input quantities are evaluated and propagated to the final results, taking correlations into account. Since the final result is normalized to the total number of events, the effect of uncertainties that are correlated across all bins is negligible. As such, only uncertainties that affect the shape of the measured distributions are significant.

The uncertainty coming from the choice of renormalization and factorization scales in the physics modeling of $\mathrm{t\bar{t}}$ events is determined by producing two additional simulated event samples. These samples are generated with both scales simultaneously varied by a factor of two up or down from their default values equal to the Q of the hard process in the event; Q is defined via $Q^2 = m_\mathrm{t}^2 + \sum p_\mathrm{T}^2$, where the sum is over all additional final-state partons in the matrix element. The effect of varying the renormalization and factorization scales in the W+jets and Z+jets samples is also considered to determine the uncertainty in the shape of this background. The uncertainty arising from the choice of parton shower matching threshold in the event generation is determined in a similar fashion, using additional samples in which the threshold is varied up or down. Uncertainties from the modeling of the hadronization are evaluated by comparing POWHEG v1 simulated samples with two different hadron shower generators (PYTHIA and HERWIG). The uncertainty owing to the choice of the PDF is determined by reweighting the simulated events and repeating the analysis using the 44 CTEQ6L PDF error sets [30]. The maximum variation is taken as the uncertainty. Simulated samples with the top quark mass varied by ± 1 GeV, which corresponds to the precision of the measured top quark mass [49], are generated to evaluate the effect of the uncertainty in this parameter. The effect of reweighting the top quark p_T spectrum in simulation, as described in Section 3, is found to have a negligible effect for low values of the kinematic event variables, and increases to 3–7% for the highest values.

Other uncertainties are associated with imperfect understanding of efficiencies, resolutions, and scales describing the detector response. The uncertainty arising from each source is estimated, and the analysis repeated with each corresponding parameter varied within its uncertainty.

The efficiencies and associated uncertainties for triggering and lepton identification are determined from data by a tag-and-probe method [50]. The probabilities for identifying and misidentifying b jets in the simulation are compared to those measured in data, and the resulting correction factors and their uncertainties are determined as a function of jet energy and quark flavor. The uncertainties in the correction factors are typically 2%.

The uncertainty in the jet energy scale (JES) is determined as a function of the jet p_T and η [41], and an uncertainty of 10% is included in the jet energy resolution (JER) [41]. The effect of this limited knowledge of the JES and JER is determined by varying the JES and JER in the

simulated samples within their uncertainties. The uncertainty in the JES and JER, as well as uncertainties in the electron, photon, tau, and muon energy scale, are propagated into the calculation of E_T^{miss}. The uncertainty in the electron and photon energy scale is 0.6% in the barrel, and 1.5% in the endcap [38]. The uncertainty in the tau lepton energy scale is estimated to be $\pm 3\%$ [51], while the effect of the uncertainty in the muon momentum measurement is found to be negligible. A 10% uncertainty is assigned to the estimate of the nonclustered energy used in the calculation of E_T^{miss} [46].

The effect of the uncertainty in the level of pileup is estimated by varying the inelastic pp cross section used in the simulation by $\pm 5\%$ [52].

The uncertainty in the normalization of the background is determined by varying the normalization of the single top, W+jets, and Z+jets processes by $\pm 30\%$, and the QCD multijet processes by $\pm 100\%$. The uncertainty in the shape of the QCD multijet distribution in the electron channel is estimated by using an alternative control region in data to determine the contribution of QCD multijet events. This uncertainty is found to have a negligible effect.

The dominant systematic effects are caused by the uncertainties in the modeling of the hadronization and the $t\bar{t}$ signal. For illustrative purposes, typical systematic uncertainties in the $\sqrt{s} = 8$ TeV results coming from each of the sources described above are presented in Table 1. The values shown for each kinematic event variable are the median uncertainties over all of the bins for that variable.

Table 1: Typical relative systematic uncertainties in percent (median values) in the normalized $t\bar{t}$ differential cross section measurement as a function of the four kinematic event variables at a center-of-mass energy of 8 TeV (combination of electron and muon channels). Typical values of the total systematic uncertainty are also shown.

Uncertainty source	Relative (%)			
	E_T^{miss}	H_T	S_T	p_T^W
Fact./Renorm. scales and matching threshold	7.6	4.0	2.6	3.3
Hadronization	4.3	5.0	8.5	3.0
PDF	0.5	0.6	0.6	0.4
Top quark mass	0.4	0.7	0.8	0.3
Top quark p_T reweighting	1.4	0.9	0.6	0.6
Lepton trigger efficiency & selection	<0.1	<0.1	<0.1	<0.1
b tagging	0.3	0.1	0.3	<0.1
Jet energy scale	0.3	0.2	0.3	<0.1
Jet energy resolution	<0.1	<0.1	<0.1	<0.1
E_T^{miss}	0.2	—	<0.1	0.1
Pileup	0.4	<0.1	0.1	0.2
Background Normalization	2.6	1.0	2.1	1.4
QCD shape	0.4	0.2	0.5	0.4
Total	9.9	8.6	9.5	4.4

7 Results

The normalized differential $t\bar{t}$ cross sections as a function of each of the kinematic event variables are shown in Figs. 3 and 4 for the $\sqrt{s} = 7$ TeV data, and in Figs. 5 and 6 for the $\sqrt{s} = 8$ TeV data. The results are also presented in Tables A.1–A.8 of Appendix A.

The data distributions in the figures are compared with the predictions from the event generators in the left-hand plots: MADGRAPH and POWHEG V2 with two different hadron shower generators, PYTHIA and HERWIG. For the $\sqrt{s} = 8$ TeV results, the predictions from the MC@NLO and POWHEG V1 generators are also shown. The effect on the predicted distributions from varying the modeling parameters (the matching threshold and renormalization scale Q^2) up and down by a factor of two for the MADGRAPH event generator is shown in the right-hand plots for the two MADGRAPH simulations. The uncertainties shown by the vertical bars on the points in the figures and given in the tables include both the statistical uncertainties and those resulting from the unfolding procedure.

The measurements at $\sqrt{s} = 7$ TeV are well described by all the event generators in the distribution of E_T^{miss}. For S_T, p_T^W, and H_T, the event generators predict a somewhat harder spectrum than seen in data. However, the POWHEG V2 + PYTHIA event generator provides a reasonable description of the H_T and S_T differential cross sections.

The results at $\sqrt{s} = 8$ TeV are generally well described by the MC@NLO and the POWHEG V2 + PYTHIA event generators. The POWHEG V2 + HERWIG event generator describes the E_T^{miss} and p_T^W distributions well. However, for H_T and S_T this event generator predicts a harder spectrum than seen in data, at both center-of-mass energies.

The MADGRAPH event generator generally predicts a harder spectrum than seen in data for all variables. The variations in matching threshold and Q^2 in the MADGRAPH event generator are not sufficient to explain this difference between the prediction and data. However, the MADGRAPH event generator provides a good description of the data after reweighting the top quark p_T spectrum, as described in Section 3. The prediction obtained from the MADGRAPH event generator after the reweighting is shown on all the plots.

8 Summary

A measurement of the normalized differential cross section of top quark pair production with respect to the four kinematic event variables E_T^{miss}, H_T, S_T, and p_T^W has been performed in pp collisions at a center-of-mass energy of 7 TeV using 5.0 fb^{-1} and at 8 TeV using 19.7 fb^{-1} of data collected by the CMS experiment.

This study confirms previous CMS findings that the observed top quark p_T spectrum is softer than predicted by the MADGRAPH, POWHEG, and MC@NLO event generators, but otherwise there is broad consistency between the MC event generators and observation. This result provides confidence in the description of $t\bar{t}$ production in the SM and its implementation in the most frequently used simulation packages.

Acknowledgments

We congratulate our colleagues in the CERN accelerator departments for the excellent performance of the LHC and thank the technical and administrative staffs at CERN and at other CMS institutes for their contributions to the success of the CMS effort. In addition, we gratefully

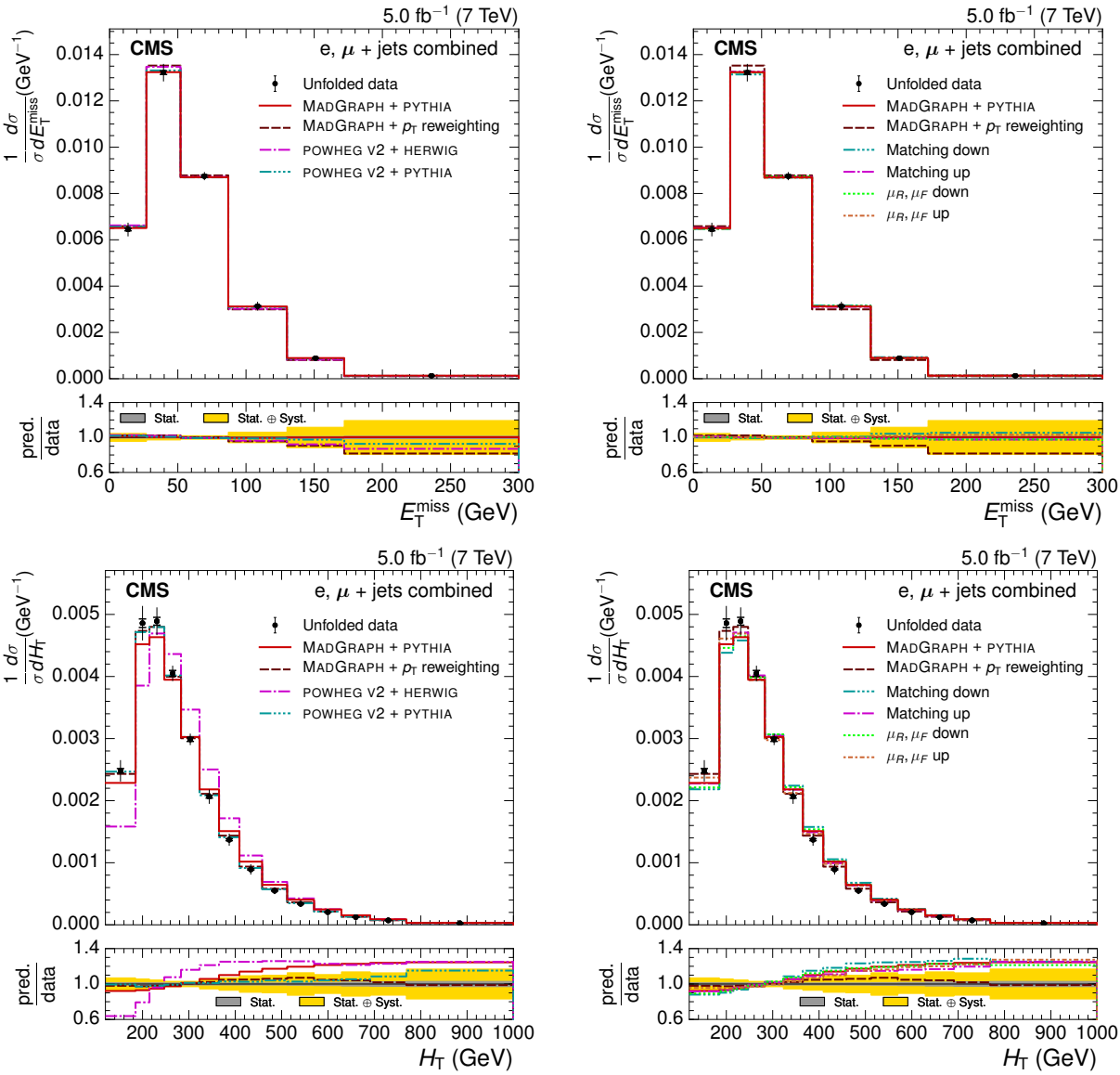

Figure 3: Normalized E_T^{miss} (top) and H_T (bottom) differential $t\bar{t}$ cross sections from the combined electron and muon data at $\sqrt{s} = 7$ TeV. The vertical bars on the data points represent the statistical and systematic uncertainties added in quadrature. The inner section of the vertical bars, denoted by the tick marks, show the statistical uncertainty. Left: comparison with different simulation event generators: MadGraph + pythia (both the default and after reweighting the top quark p_T spectrum), powheg v2 + herwig, and powheg v2 + pythia. Right: comparison with predictions from the MadGraph + pythia event generator found by varying the matching threshold and renormalization scales (μ_R, μ_F) up and down by a factor of two. The lower plots show the ratio of the predictions to the data, with the statistical and total uncertainties in the ratios indicated by the two shaded bands.

acknowledge the computing centers and personnel of the Worldwide LHC Computing Grid for delivering so effectively the computing infrastructure essential to our analyses. Finally, we acknowledge the enduring support for the construction and operation of the LHC and the CMS detector provided by the following funding agencies: BMWFW and FWF (Austria); FNRS and FWO (Belgium); CNPq, CAPES, FAPERJ, and FAPESP (Brazil); MES (Bulgaria); CERN;

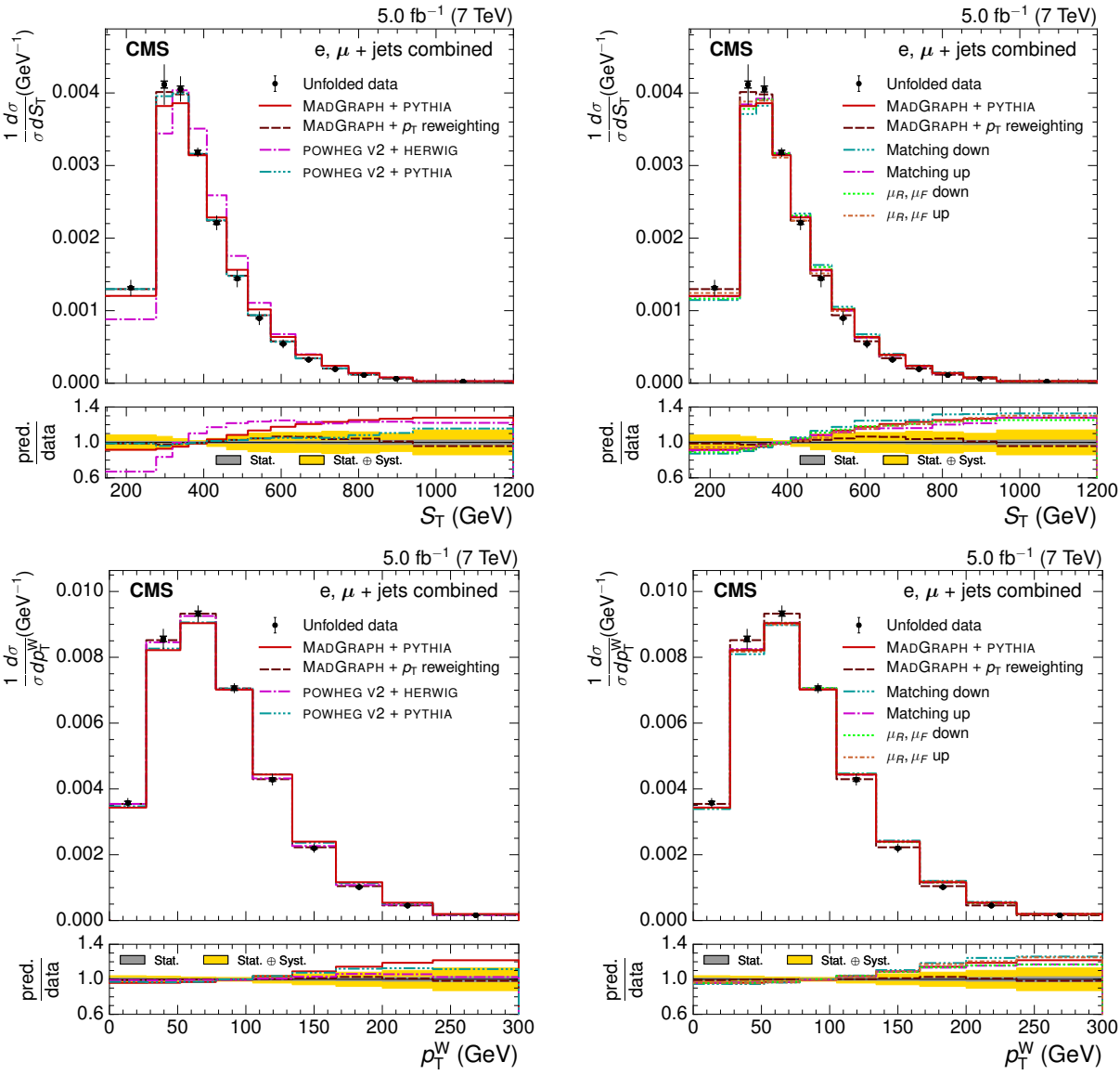

Figure 4: Normalized S_T (top) and p_T^W (bottom) differential $t\bar{t}$ cross sections from combined electron and muon data at $\sqrt{s} = 7$ TeV. The vertical bars on the data points represent the statistical and systematic uncertainties added in quadrature. The inner section of the vertical bars, denoted by the tick marks, show the statistical uncertainty. Left: comparison with different simulation event generators: MADGRAPH + PYTHIA (both the default and after reweighting the top quark p_T spectrum), POWHEG V2 + HERWIG, and POWHEG V2 + PYTHIA. Right: comparison with predictions from the MADGRAPH + PYTHIA event generator found by varying the matching threshold and renormalization scales (μ_R, μ_F) up and down by a factor of two. The lower plots show the ratio of the predictions to the data, with the statistical and total uncertainties in the ratios indicated by the two shaded bands.

CAS, MoST, and NSFC (China); COLCIENCIAS (Colombia); MSES and CSF (Croatia); RPF (Cyprus); SENESCYT (Ecuador); MoER, ERC IUT and ERDF (Estonia); Academy of Finland, MEC, and HIP (Finland); CEA and CNRS/IN2P3 (France); BMBF, DFG, and HGF (Germany); GSRT (Greece); OTKA and NIH (Hungary); DAE and DST (India); IPM (Iran); SFI (Ireland); INFN (Italy); MSIP and NRF (Republic of Korea); LAS (Lithuania); MOE and UM (Malaysia);

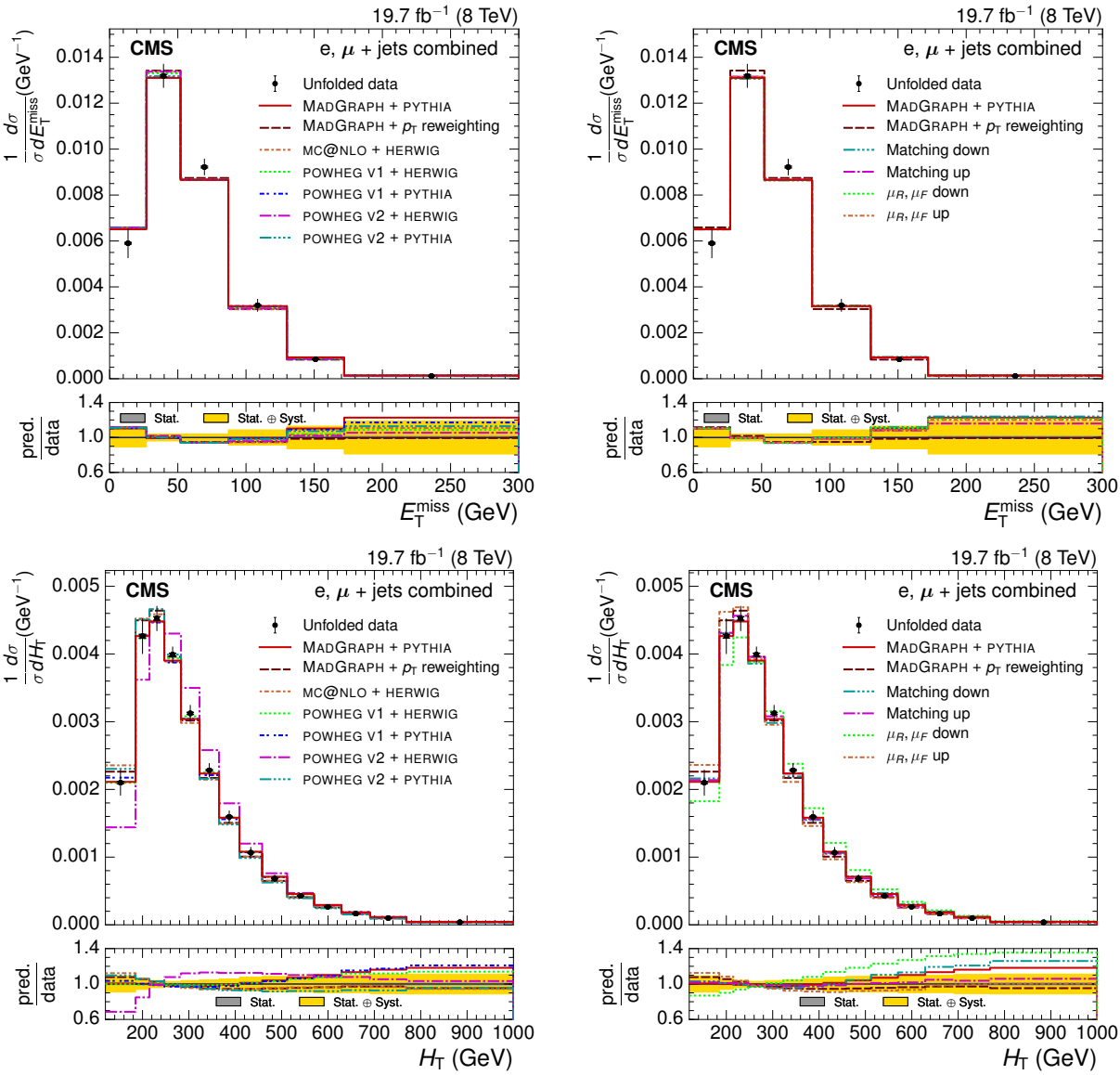

Figure 5: Normalized E_T^{miss} (top) and H_T (bottom) differential $t\bar{t}$ cross sections from combined electron and muon data at $\sqrt{s} = 8$ TeV. The vertical bars on the data points represent the statistical and systematic uncertainties added in quadrature. The inner section of the vertical bars, denoted by the tick marks, show the statistical uncertainty. Left: comparison with different simulation event generators: MadGraph + pythia (both the default and after reweighting the top quark p_T spectrum), MC@NLO + Herwig, powheg v1 + Herwig, powheg v1 + pythia, powheg v2 + Herwig, and powheg v2 + pythia. Right: comparison with predictions from the pythia event generator found by varying the matching threshold and renormalization scales (μ_R, μ_F) up and down by a factor of two. The lower plots show the ratio of the predictions to the data, with the statistical and total uncertainties in the ratios indicated by the two shaded bands.

BUAP, CINVESTAV, CONACYT, LNS, SEP, and UASLP-FAI (Mexico); MBIE (New Zealand); PAEC (Pakistan); MSHE and NSC (Poland); FCT (Portugal); JINR (Dubna); MON, RosAtom, RAS and RFBR (Russia); MESTD (Serbia); SEIDI and CPAN (Spain); Swiss Funding Agencies (Switzerland); MST (Taipei); ThEPCenter, IPST, STAR and NSTDA (Thailand); TUBITAK and

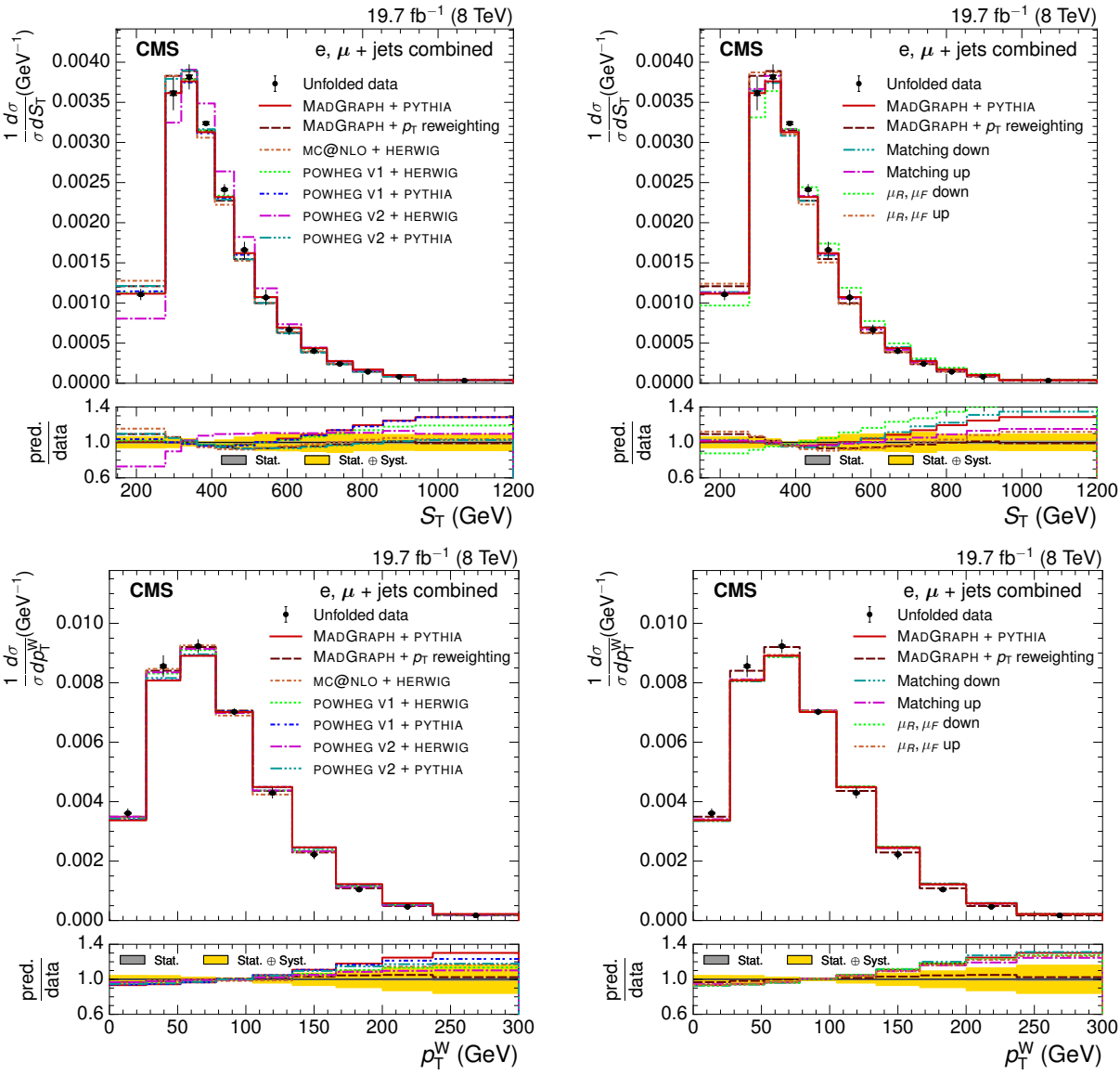

Figure 6: Normalized S_T (top) and p_T^W (bottom) differential $t\bar{t}$ cross sections from combined electron and muon data at $\sqrt{s} = 8$ TeV. The vertical bars on the data points represent the statistical and systematic uncertainties added in quadrature. The inner section of the vertical bars, denoted by the tick marks, show the statistical uncertainty. Left: comparison with different simulation event generators: MADGRAPH + PYTHIA (both the default and after reweighting the top quark p_T spectrum), MC@NLO + HERWIG, POWHEG V1 + HERWIG, POWHEG V1 + PYTHIA, POWHEG V2 + HERWIG, and POWHEG V2 + PYTHIA. Right: comparison with predictions from the MADGRAPH + PYTHIA event generator found by varying the matching threshold and renormalization scales (μ_R, μ_F) up and down by a factor of two. The lower plots show the ratio of the predictions to the data, with the statistical and total uncertainties in the ratios indicated by the two shaded bands.

TAEK (Turkey); NASU and SFFR (Ukraine); STFC (United Kingdom); DOE and NSF (USA).

Individuals have received support from the Marie-Curie program and the European Research Council and EPLANET (European Union); the Leventis Foundation; the A. P. Sloan Founda-

tion; the Alexander von Humboldt Foundation; the Belgian Federal Science Policy Office; the Fonds pour la Formation à la Recherche dans l'Industrie et dans l'Agriculture (FRIA-Belgium); the Agentschap voor Innovatie door Wetenschap en Technologie (IWT-Belgium); the Ministry of Education, Youth and Sports (MEYS) of the Czech Republic; the Council of Science and Industrial Research, India; the HOMING PLUS program of the Foundation for Polish Science, cofinanced from European Union, Regional Development Fund, the Mobility Plus program of the Ministry of Science and Higher Education, the OPUS program contract 2014/13/B/ST2/02543 and contract Sonata-bis DEC-2012/07/E/ST2/01406 of the National Science Center (Poland); the Thalis and Aristeia programmes cofinanced by EU-ESF and the Greek NSRF; the National Priorities Research Program by Qatar National Research Fund; the Programa Clarín-COFUND del Principado de Asturias; the Rachadapisek Sompot Fund for Postdoctoral Fellowship, Chulalongkorn University and the Chulalongkorn Academic into Its 2nd Century Project Advancement Project (Thailand); and the Welch Foundation, contract C-1845.

References

[1] CMS Collaboration, "The CMS experiment at the CERN LHC", *JINST* **3** (2008) S08004, doi:10.1088/1748-0221/3/08/S08004.

[2] CDF Collaboration, "First measurement of the $\mathrm{t\bar{t}}$ differential cross section $\mathrm{d}\sigma/\mathrm{d}M_{\mathrm{t\bar{t}}}$ in $\mathrm{p\bar{p}}$ collisions at $\sqrt{s} = 1.96\,\mathrm{TeV}$", *Phys. Rev. Lett.* **102** (2009) 222003, doi:10.1103/PhysRevLett.102.222003, arXiv:0903.2850.

[3] D0 Collaboration, "Measurement of differential $\mathrm{t\bar{t}}$ production cross sections in $\mathrm{p\bar{p}}$ collisions", *Phys. Rev. D* **90** (2014) 092006, doi:10.1103/PhysRevD.90.092006, arXiv:1401.5785.

[4] CMS Collaboration, "Measurement of differential top-quark pair production cross sections in pp colisions at $\sqrt{s} = 7\,\mathrm{TeV}$", *Eur. Phys. J. C* **73** (2013) 2339, doi:10.1140/epjc/s10052-013-2339-4, arXiv:1211.2220.

[5] CMS Collaboration, "Measurement of the differential cross section for top quark pair production in pp collisions at $\sqrt{s} = 8\,\mathrm{TeV}$", *Eur. Phys. J. C* **75** (2015) 542, doi:10.1140/epjc/s10052-015-3709-x, arXiv:1505.04480.

[6] CMS Collaboration, "Measurement of $\mathrm{t\bar{t}}$ production with additional jet activity, including b quark jets, in the dilepton channel using pp collisions at $\sqrt{s} = 8\,\mathrm{TeV}$", (2016). arXiv:1510.03072. Accepted in *Eur. Phys. J. C*.

[7] CMS Collaboration, "Measurement of the differential $\mathrm{t\bar{t}}$ production cross section for high-p_{T} top quarks in e/μ+jets final states at 8 TeV", CMS Physics Analysis Summary CMS-PAS-TOP-14-012, CERN, 2015.

[8] ATLAS Collaboration, "Differential $\mathrm{t\bar{t}}$ cross-section measurements as a function of observables constructed from final-state particles using pp collisions at $\sqrt{s} = 7\,\mathrm{TeV}$ in the ATLAS detector", *JHEP* **06** (2015) 100, doi:10.1007/JHEP06(2015)100, arXiv:1502.05923.

[9] ATLAS Collaboration, "Measurement of the differential cross-section of highly boosted top quarks as a function of their transverse momentum in $\sqrt{s} = 8\,\mathrm{TeV}$ proton-proton collisions using the ATLAS detector", *Phys. Rev. D* **93** (2016) 032009, doi:10.1103/PhysRevD.93.032009, arXiv:1510.03818.

[10] J. Alwall et al., "The automated computation of tree-level and next-to-leading order differential cross sections, and their matching to parton shower simulations", *JHEP* **07** (2014) 079, doi:10.1007/JHEP07(2014)079, arXiv:1405.0301.

[11] M. Czakon and A. Mitov, "Top++: a program for the calculation of the top-pair cross-section at hadron colliders", *Comput. Phys. Commun.* **185** (2014) 2930, doi:10.1016/j.cpc.2014.06.021, arXiv:1112.5675.

[12] M. Botje et al., "The PDF4LHC Working Group interim recommendations", (2011). arXiv:1101.0538.

[13] S. Alekhin et al., "The PDF4LHC Working Group interim report", (2011). arXiv:1101.0536.

[14] A. D. Martin, W. J. Stirling, R. S. Thorne, and G. Watt, "Uncertainties on α_S in global PDF analyses and implications for predicted hadronic cross sections", *Eur. Phys. J. C* **64** (2009) 653, doi:10.1140/epjc/s10052-009-1164-2, arXiv:0905.3531.

[15] J. Gao et al., "CT10 next-to-next-to-leading order global analysis of QCD", *Phys. Rev. D* **89** (2014) 033009, doi:10.1103/PhysRevD.89.033009, arXiv:1302.6246.

[16] NNPDF Collaboration, "Parton distributions with LHC data", *Nucl. Phys. B* **867** (2013) 244, doi:10.1016/j.nuclphysb.2012.10.003, arXiv:1207.1303.

[17] T. Sjöstrand, S. Mrenna, and P. Skands, "PYTHIA 6.4 physics and manual", *JHEP* **05** (2006) 026, doi:10.1088/1126-6708/2006/05/026, arXiv:hep-ph/0603175.

[18] S. Höche et al., "Matching parton showers and matrix elements", in *HERA and the LHC: A Workshop on the implications of HERA for LHC physics: Proceedings Part A*. 2006. arXiv:hep-ph/0602031.

[19] GEANT4 Collaboration, "GEANT4—a simulation toolkit", *Nucl. Instrum. Meth. A* **506** (2003) 250, doi:10.1016/S0168-9002(03)01368-8.

[20] P. Nason, "A new method for combining NLO QCD with shower Monte Carlo algorithms", *JHEP* **11** (2004) 040, doi:10.1088/1126-6708/2004/11/040, arXiv:hep-ph/0409146.

[21] S. Frixione, P. Nason, and C. Oleari, "Matching NLO QCD computations with parton shower simulations: the POWHEG method", *JHEP* **11** (2007) 070, doi:10.1088/1126-6708/2007/11/070, arXiv:0709.2092.

[22] S. Alioli, P. Nason, C. Oleari, and E. Re, "A general framework for implementing NLO calculations in shower Monte Carlo programs: the POWHEG BOX", *JHEP* **06** (2010) 043, doi:10.1007/JHEP06(2010)043, arXiv:1002.2581.

[23] S. Frixione and B. R. Webber, "Matching NLO QCD computations and parton shower simulations", *JHEP* **06** (2002) 029, doi:10.1088/1126-6708/2002/06/029, arXiv:hep-ph/0204244.

[24] G. Corcella et al., "HERWIG 6: an event generator for hadron emission reactions with interfering gluons (including supersymmetric processes)", *JHEP* **01** (2001) 010, doi:10.1088/1126-6708/2001/01/010, arXiv:hep-ph/0011363.

[25] S. Alioli, P. Nason, C. Oleari, and E. Re, "NLO single-top production matched with shower in POWHEG: s- and t-channel contributions", *JHEP* **09** (2009) 111, doi:10.1088/1126-6708/2009/09/111, arXiv:0907.4076. [Erratum: doi:10.1007/JHEP02(2010)011].

[26] E. Re, "Single-top Wt-channel production matched with parton showers using the POWHEG method", *Eur. Phys. J. C* **71** (2011) 1547, doi:10.1140/epjc/s10052-011-1547-z, arXiv:1009.2450.

[27] K. Melnikov and F. Petriello, "Electroweak gauge boson production at hadron colliders through $\mathcal{O}(\alpha_s^2)$", *Phys. Rev. D* **74** (2006) 114017, doi:10.1103/PhysRevD.74.114017, arXiv:hep-ph/0609070.

[28] K. Melnikov and F. Petriello, "W boson production cross section at the large hadron collider with $\mathcal{O}(\alpha_s^2)$ corrections", *Phys. Rev. Lett.* **96** (2006) 231803, doi:10.1103/PhysRevLett.96.231803.

[29] N. Kidonakis, "NNLL threshold resummation for top-pair and single-top production", *Phys. Part. Nucl.* **45** (2014) 714, doi:10.1134/S1063779614040091, arXiv:1210.7813.

[30] J. Pumplin et al., "New generation of parton distributions with uncertainties from global QCD analysis", *JHEP* **07** (2002) 012, doi:10.1088/1126-6708/2002/07/012, arXiv:hep-ph/0201195.

[31] H.-L. Lai et al., "New parton distributions for collider physics", *Phys. Rev. D* **82** (2010) 074024, doi:10.1103/PhysRevD.82.074024, arXiv:1007.2241.

[32] CMS Collaboration, "Measurement of the underlying event activity at the LHC with $\sqrt{s} = 7$ TeV and comparison with $\sqrt{s} = 0.9$ TeV", *JHEP* **09** (2011) 109, doi:10.1007/JHEP09(2011)109, arXiv:1107.0330.

[33] ATLAS Collaboration, "ATLAS tunes of PYTHIA 6 and Pythia 8 for MC11", Technical Report ATL-PHYS-PUB-2011-009, CERN, 2011.

[34] P. Bartalini, R. Chierici, and A. de Roeck, "Guidelines for the estimation of theoretical uncertainties at the LHC", Technical Report CMS-NOTE-2005-013, CERN, 2005.

[35] CMS Collaboration, "Description and performance of track and primary-vertex reconstruction with the CMS tracker", *JINST* **9** (2014) P10009, doi:10.1088/1748-0221/9/10/P10009, arXiv:1405.6569.

[36] CMS Collaboration, "Particle-flow event reconstruction in CMS and performance for jets, taus, and $E_{\mathrm{T}}^{\mathrm{miss}}$", CMS Physics Analysis Summary CMS-PAS-PFT-09-001, CERN, 2009.

[37] CMS Collaboration, "Commissioning of the particle-flow reconstruction in minimum-bias and jet events from pp collisions at 7 TeV", CMS Physics Analysis Summary CMS-PAS-PFT-10-002, CERN, 2010.

[38] CMS Collaboration, "Performance of electron reconstruction and selection with the CMS detector in proton-proton collisions at $\sqrt{s} = 8$ TeV", *JINST* **10** (2015) P06005, doi:10.1088/1748-0221/10/06/P06005, arXiv:1502.02701.

[39] CMS Collaboration, "Performance of CMS muon reconstruction in pp collision events at $\sqrt{s} = 7$ TeV", *JINST* **7** (2012) P10002, doi:10.1088/1748-0221/7/10/P10002, arXiv:1206.4071.

[40] M. Cacciari, G. P. Salam, and G. Soyez, "The anti-k_t jet clustering algorithm", *JHEP* **04** (2008) 063, doi:10.1088/1126-6708/2008/04/063, arXiv:hep-ph/0802.1189.

[41] CMS Collaboration, "Determination of jet energy calibration and transverse momentum resolution in CMS", *JINST* **6** (2011) P11002, doi:10.1088/1748-0221/6/11/P11002, arXiv:1107.4277.

[42] M. Cacciari, G. P. Salam, and G. Soyez, "The catchment area of jets", *JHEP* **04** (2008) 005, doi:10.1088/1126-6708/2008/04/005, arXiv:0802.1188.

[43] M. Cacciari and G. P. Salam, "Pileup subtraction using jet areas", *Phys. Lett. B* **659** (2008) 119, doi:10.1016/j.physletb.2007.09.077, arXiv:0707.1378.

[44] CMS Collaboration, "Measurement of the ratio of the inclusive 3-jet cross section to the inclusive 2-jet cross section in pp collisions at $\sqrt{s} = 7$ TeV and first determination of the strong coupling constant in the TeV range", *Eur. Phys. J. C* **73** (2013) 2604, doi:10.1140/epjc/s10052-013-2604-6, arXiv:1304.7498.

[45] CMS Collaboration, "Identification of b-quark jets with the CMS experiment", *JINST* **8** (2013) P04013, doi:10.1088/1748-0221/8/04/P04013, arXiv:1211.4462.

[46] CMS Collaboration, "Performance of the CMS missing transverse momentum reconstruction in pp data at $\sqrt{s} = 8$ TeV", *JINST* **10** (2015) P02006, doi:10.1088/1748-0221/10/02/P02006, arXiv:1411.0511.

[47] A. Höcker and V. Kartvelishvili, "SVD approach to data unfolding", *Nucl. Instrum. Meth. A* **372** (1996) 469, doi:10.1016/0168-9002(95)01478-0, arXiv:hep-ph/9509307.

[48] T. Adye, "Unfolding algorithms and tests using RooUnfold", in *Proceedings of the PHYSTAT 2011 Workshop, CERN-2011-006*, p. 313. 2011. arXiv:1105.1160.

[49] Particle Data Group, K. A. Olive et al., "Review of Particle Physics", *Chin. Phys. C* **38** (2014) 090001, doi:10.1088/1674-1137/38/9/090001.

[50] CMS Collaboration, "Measurements of inclusive W and Z cross sections in pp collisions at $\sqrt{s} = 7$ TeV", *JHEP* **01** (2011) 080, doi:10.1007/JHEP01(2011)080, arXiv:1012.2466.

[51] CMS Collaboration, "Evidence for the 125 GeV Higgs boson decaying to a pair of τ leptons", *JHEP* **05** (2014) 104, doi:10.1007/JHEP05(2014)104, arXiv:1401.5041.

[52] CMS Collaboration, "Measurement of the inelastic proton-proton cross section at $\sqrt{s} = 7$ TeV", *Phys. Lett. B* **722** (2013) 5, doi:10.1016/j.physletb.2013.03.024, arXiv:1210.6718.

A Additional tables

The measured values of the $t\bar{t}$ differential cross sections as a function of E_T^{miss}, H_T, S_T, and p_T^W for $\sqrt{s} = 7$ TeV and $\sqrt{s} = 8$ TeV are given in the tables below, along with their statistical, systematic, and total uncertainties.

Table A.1: Normalized $t\bar{t}$ differential cross section measurements with respect to the E_T^{miss} variable at a center-of-mass energy of 7 TeV (combination of electron and muon channels). The rightmost three columns show the relative uncertainties on the measured values, in percent. The statistical and systematic uncertainties are listed separately, and are combined in quadrature to give the overall relative uncertainty.

E_T^{miss} (GeV)	$1/\sigma\, d\sigma/dE_T^{miss}$ (GeV^{-1})	± stat. (%)	± syst. (%)	Rel. uncert. (%)
0–27	6.44×10^{-3}	0.83	4.5	4.6
27–52	1.32×10^{-2}	0.60	2.8	2.9
52–87	8.75×10^{-3}	0.58	1.9	2.0
87–130	3.14×10^{-3}	0.80	6.0	6.0
130–172	8.93×10^{-4}	1.1	12	12
172–300	1.32×10^{-4}	1.4	19	19

Table A.2: Normalized $t\bar{t}$ differential cross section measurements with respect to the H_T variable at a center-of-mass energy of 7 TeV (combination of electron and muon channels). The rightmost three columns show the relative uncertainties on the measured values, in percent. The statistical and systematic uncertainties are listed separately, and are combined in quadrature to give the overall relative uncertainty.

H_T (GeV)	$1/\sigma\, d\sigma/dH_T$ (GeV^{-1})	± stat. (%)	± syst. (%)	Rel. uncert. (%)
120–185	2.48×10^{-3}	1.5	6.8	6.9
185–215	4.86×10^{-3}	1.4	5.5	5.7
215–247	4.89×10^{-3}	1.3	4.4	4.6
247–283	4.05×10^{-3}	1.2	2.8	3.1
283–323	2.99×10^{-3}	1.1	2.9	3.1
323–365	2.06×10^{-3}	1.1	5.4	5.6
365–409	1.37×10^{-3}	1.1	7.0	7.1
409–458	8.93×10^{-4}	1.1	9.3	9.4
458–512	5.49×10^{-4}	1.2	9.9	10
512–570	3.38×10^{-4}	1.4	13	13
570–629	2.04×10^{-4}	1.8	10	11
629–691	1.25×10^{-4}	2.2	14	14
691–769	7.20×10^{-5}	2.7	12	13
769–1000	2.51×10^{-5}	3.0	17	17

Table A.3: Normalized $t\bar{t}$ differential cross section measurements with respect to the S_T variable at a center-of-mass energy of 7 TeV (combination of electron and muon channels). The rightmost three columns show the relative uncertainties on the measured values, in percent. The statistical and systematic uncertainties are listed separately, and are combined in quadrature to give the overall relative uncertainty.

S_T (GeV)	$1/\sigma\, d\sigma/dS_T$ (GeV^{-1})	$\pm$ stat. (%)	$\pm$ syst. (%)	Rel. uncert. (%)
146–277	1.31×10^{-3}	1.2	8.4	8.5
277–319	4.12×10^{-3}	1.1	6.7	6.8
319–361	4.05×10^{-3}	1.0	4.2	4.3
361–408	3.18×10^{-3}	0.91	1.8	2.0
408–459	2.21×10^{-3}	0.93	4.5	4.6
459–514	1.44×10^{-3}	1.0	8.1	8.2
514–573	8.96×10^{-4}	1.1	10	11
573–637	5.42×10^{-4}	1.2	11	11
637–705	3.25×10^{-4}	1.3	11	11
705–774	1.95×10^{-4}	1.6	12	13
774–854	1.13×10^{-4}	1.9	12	12
854–940	6.32×10^{-5}	2.3	10	10
940–1200	2.26×10^{-5}	2.7	14	14

Table A.4: Normalized $t\bar{t}$ differential cross section measurements with respect to the p_T^W variable at a center-of-mass energy of 7 TeV (combination of electron and muon channels). The rightmost three columns show the relative uncertainties on the measured values, in percent. The statistical and systematic uncertainties are listed separately, and are combined in quadrature to give the overall relative uncertainty.

p_T^W (GeV)	$1/\sigma\, d\sigma/dp_T^W$ (GeV^{-1})	$\pm$ stat. (%)	$\pm$ syst. (%)	Rel. uncert. (%)
0–27	3.58×10^{-3}	1.3	3.8	4.1
27–52	8.56×10^{-3}	0.96	3.4	3.6
52–78	9.33×10^{-3}	0.81	2.5	2.6
78–105	7.06×10^{-3}	0.96	1.9	2.1
105–134	4.28×10^{-3}	1.2	4.1	4.2
134–166	2.20×10^{-3}	1.3	6.1	6.2
166–200	1.02×10^{-3}	1.6	8.0	8.1
200–237	4.56×10^{-4}	2.2	9.9	10
237–300	1.63×10^{-4}	2.9	13	13

Table A.5: Normalized $t\bar{t}$ differential cross section measurements with respect to the E_T^{miss} variable at a center-of-mass energy of 8 TeV (combination of electron and muon channels). The rightmost three columns show the relative uncertainties on the measured values, in percent. The statistical and systematic uncertainties are listed separately, and are combined in quadrature to give the overall relative uncertainty.

E_T^{miss} (GeV)	$1/\sigma\, d\sigma/dE_T^{miss}$ (GeV^{-1})	± stat. (%)	± syst. (%)	Rel. uncert. (%)
0–27	5.90×10^{-3}	0.59	11	11
27–52	1.32×10^{-2}	0.36	3.9	3.9
52–87	9.22×10^{-3}	0.40	3.9	3.9
87–130	3.20×10^{-3}	0.55	8.6	8.7
130–172	8.46×10^{-4}	0.81	13	13
172–300	1.18×10^{-4}	1.3	19	19

Table A.6: Normalized $t\bar{t}$ differential cross section measurements with respect to the H_T variable at a center-of-mass energy of 8 TeV (combination of electron and muon channels). The rightmost three columns show the relative uncertainties on the measured values, in percent. The statistical and systematic uncertainties are listed separately, and are combined in quadrature to give the overall relative uncertainty.

H_T (GeV)	$1/\sigma\, d\sigma/dH_T$ (GeV^{-1})	± stat. (%)	± syst. (%)	Rel. uncert. (%)
120–185	2.10×10^{-3}	0.68	9.1	9.1
185–215	4.26×10^{-3}	0.65	6.1	6.2
215–247	4.52×10^{-3}	0.57	4.1	4.1
247–283	3.99×10^{-3}	0.50	2.9	3.0
283–323	3.12×10^{-3}	0.46	4.0	4.0
323–365	2.28×10^{-3}	0.44	4.5	4.6
365–409	1.60×10^{-3}	0.44	5.8	5.8
409–458	1.07×10^{-3}	0.43	7.9	7.9
458–512	6.83×10^{-4}	0.45	8.6	8.6
512–570	4.26×10^{-4}	0.51	9.0	9.0
570–629	2.66×10^{-4}	0.65	9.9	9.9
629–691	1.64×10^{-4}	0.82	9.7	9.7
691–769	9.93×10^{-5}	0.99	11	11
769–1000	3.78×10^{-5}	1.1	11	11

Table A.7: Normalized $t\bar{t}$ differential cross section measurements with respect to the S_T variable at a center-of-mass energy of 8 TeV (combination of electron and muon channels). The rightmost three columns show the relative uncertainties on the measured values, in percent. The statistical and systematic uncertainties are listed separately, and are combined in quadrature to give the overall relative uncertainty.

S_T (GeV)	$1/\sigma\, d\sigma/dS_T$ (GeV^{-1})	± stat. (%)	± syst. (%)	Rel. uncert. (%)
146–277	1.10×10^{-3}	0.84	6.3	6.3
277–319	3.61×10^{-3}	0.71	5.8	5.9
319–361	3.82×10^{-3}	0.54	4.1	4.1
361–408	3.24×10^{-3}	0.46	0.80	0.92
408–459	2.41×10^{-3}	0.48	2.8	2.9
459–514	1.66×10^{-3}	0.57	6.1	6.1
514–573	1.07×10^{-3}	0.69	9.0	9.1
573–637	6.65×10^{-4}	0.74	9.6	9.6
637–705	4.03×10^{-4}	0.71	10	10
705–774	2.43×10^{-4}	0.73	11	11
774–854	1.44×10^{-4}	0.88	9.3	9.4
854–940	8.21×10^{-5}	1.2	8.9	9.0
940–1200	3.15×10^{-5}	1.5	9.2	9.4

Table A.8: Normalized $t\bar{t}$ differential cross section measurements with respect to the p_T^W variable at a center-of-mass energy of 8 TeV (combination of electron and muon channels). The rightmost three columns show the relative uncertainties on the measured values, in percent. The statistical and systematic uncertainties are listed separately, and are combined in quadrature to give the overall relative uncertainty.

p_T^W (GeV)	$1/\sigma\, d\sigma/dp_T^W$ (GeV^{-1})	± stat. (%)	± syst. (%)	Rel. uncert. (%)
0–27	3.61×10^{-3}	0.54	4.4	4.4
27–52	8.56×10^{-3}	0.40	4.3	4.3
52–78	9.23×10^{-3}	0.34	2.5	2.5
78–105	7.02×10^{-3}	0.40	1.6	1.6
105–134	4.29×10^{-3}	0.50	4.3	4.3
134–166	2.22×10^{-3}	0.55	7.1	7.1
166–200	1.04×10^{-3}	0.67	9.6	9.6
200–237	4.66×10^{-4}	0.94	13	13
237–300	1.69×10^{-4}	1.2	16	16

B The CMS Collaboration

Yerevan Physics Institute, Yerevan, Armenia
V. Khachatryan, A.M. Sirunyan, A. Tumasyan

Institut für Hochenergiephysik der OeAW, Wien, Austria
W. Adam, E. Asilar, T. Bergauer, J. Brandstetter, E. Brondolin, M. Dragicevic, J. Erö, M. Flechl, M. Friedl, R. Frühwirth[1], V.M. Ghete, C. Hartl, N. Hörmann, J. Hrubec, M. Jeitler[1], V. Knünz, A. König, M. Krammer[1], I. Krätschmer, D. Liko, T. Matsushita, I. Mikulec, D. Rabady[2], B. Rahbaran, H. Rohringer, J. Schieck[1], R. Schöfbeck, J. Strauss, W. Treberer-Treberspurg, W. Waltenberger, C.-E. Wulz[1]

National Centre for Particle and High Energy Physics, Minsk, Belarus
V. Mossolov, N. Shumeiko, J. Suarez Gonzalez

Universiteit Antwerpen, Antwerpen, Belgium
S. Alderweireldt, T. Cornelis, E.A. De Wolf, X. Janssen, A. Knutsson, J. Lauwers, S. Luyckx, S. Ochesanu, R. Rougny, M. Van De Klundert, H. Van Haevermaet, P. Van Mechelen, N. Van Remortel, A. Van Spilbeeck

Vrije Universiteit Brussel, Brussel, Belgium
S. Abu Zeid, F. Blekman, J. D'Hondt, N. Daci, I. De Bruyn, K. Deroover, N. Heracleous, J. Keaveney, S. Lowette, L. Moreels, A. Olbrechts, Q. Python, D. Strom, S. Tavernier, W. Van Doninck, P. Van Mulders, G.P. Van Onsem, I. Van Parijs

Université Libre de Bruxelles, Bruxelles, Belgium
P. Barria, C. Caillol, B. Clerbaux, G. De Lentdecker, H. Delannoy, G. Fasanella, L. Favart, A.P.R. Gay, A. Grebenyuk, G. Karapostoli, T. Lenzi, A. Léonard, T. Maerschalk, A. Marinov, L. Perniè, A. Randle-conde, T. Reis, T. Seva, C. Vander Velde, P. Vanlaer, R. Yonamine, F. Zenoni, F. Zhang[3]

Ghent University, Ghent, Belgium
K. Beernaert, L. Benucci, A. Cimmino, S. Crucy, D. Dobur, A. Fagot, G. Garcia, M. Gul, J. Mccartin, A.A. Ocampo Rios, D. Poyraz, D. Ryckbosch, S. Salva, M. Sigamani, N. Strobbe, M. Tytgat, W. Van Driessche, E. Yazgan, N. Zaganidis

Université Catholique de Louvain, Louvain-la-Neuve, Belgium
S. Basegmez, C. Beluffi[4], O. Bondu, S. Brochet, G. Bruno, R. Castello, A. Caudron, L. Ceard, G.G. Da Silveira, C. Delaere, D. Favart, L. Forthomme, A. Giammanco[5], J. Hollar, A. Jafari, P. Jez, M. Komm, V. Lemaitre, A. Mertens, C. Nuttens, L. Perrini, A. Pin, K. Piotrzkowski, A. Popov[6], L. Quertenmont, M. Selvaggi, M. Vidal Marono

Université de Mons, Mons, Belgium
N. Beliy, G.H. Hammad

Centro Brasileiro de Pesquisas Fisicas, Rio de Janeiro, Brazil
W.L. Aldá Júnior, G.A. Alves, L. Brito, M. Correa Martins Junior, M. Hamer, C. Hensel, C. Mora Herrera, A. Moraes, M.E. Pol, P. Rebello Teles

Universidade do Estado do Rio de Janeiro, Rio de Janeiro, Brazil
E. Belchior Batista Das Chagas, W. Carvalho, J. Chinellato[7], A. Custódio, E.M. Da Costa, D. De Jesus Damiao, C. De Oliveira Martins, S. Fonseca De Souza, L.M. Huertas Guativa, H. Malbouisson, D. Matos Figueiredo, L. Mundim, H. Nogima, W.L. Prado Da Silva, A. Santoro, A. Sznajder, E.J. Tonelli Manganote[7], A. Vilela Pereira

Universidade Estadual Paulista [a], Universidade Federal do ABC [b], São Paulo, Brazil
S. Ahuja[a], C.A. Bernardes[b], A. De Souza Santos[b], S. Dogra[a], T.R. Fernandez Perez Tomei[a], E.M. Gregores[b], P.G. Mercadante[b], C.S. Moon[a,8], S.F. Novaes[a], Sandra S. Padula[a], D. Romero Abad, J.C. Ruiz Vargas

Institute for Nuclear Research and Nuclear Energy, Sofia, Bulgaria
A. Aleksandrov, R. Hadjiiska, P. Iaydjiev, M. Rodozov, S. Stoykova, G. Sultanov, M. Vutova

University of Sofia, Sofia, Bulgaria
A. Dimitrov, I. Glushkov, L. Litov, B. Pavlov, P. Petkov

Institute of High Energy Physics, Beijing, China
M. Ahmad, J.G. Bian, G.M. Chen, H.S. Chen, M. Chen, T. Cheng, R. Du, C.H. Jiang, R. Plestina[9], F. Romeo, S.M. Shaheen, J. Tao, C. Wang, Z. Wang, H. Zhang

State Key Laboratory of Nuclear Physics and Technology, Peking University, Beijing, China
C. Asawatangtrakuldee, Y. Ban, Q. Li, S. Liu, Y. Mao, S.J. Qian, D. Wang, Z. Xu, W. Zou

Universidad de Los Andes, Bogota, Colombia
C. Avila, A. Cabrera, L.F. Chaparro Sierra, C. Florez, J.P. Gomez, B. Gomez Moreno, J.C. Sanabria

University of Split, Faculty of Electrical Engineering, Mechanical Engineering and Naval Architecture, Split, Croatia
N. Godinovic, D. Lelas, I. Puljak, P.M. Ribeiro Cipriano

University of Split, Faculty of Science, Split, Croatia
Z. Antunovic, M. Kovac

Institute Rudjer Boskovic, Zagreb, Croatia
V. Brigljevic, K. Kadija, J. Luetic, S. Micanovic, L. Sudic

University of Cyprus, Nicosia, Cyprus
A. Attikis, G. Mavromanolakis, J. Mousa, C. Nicolaou, F. Ptochos, P.A. Razis, H. Rykaczewski

Charles University, Prague, Czech Republic
M. Bodlak, M. Finger[10], M. Finger Jr.[10]

Academy of Scientific Research and Technology of the Arab Republic of Egypt, Egyptian Network of High Energy Physics, Cairo, Egypt
M. El Sawy[11,12], E. El-khateeb[13], T. Elkafrawy[13], A. Mohamed[14], Y. Mohammed[15], E. Salama[13,12]

National Institute of Chemical Physics and Biophysics, Tallinn, Estonia
B. Calpas, M. Kadastik, M. Murumaa, M. Raidal, A. Tiko, C. Veelken

Department of Physics, University of Helsinki, Helsinki, Finland
P. Eerola, J. Pekkanen, M. Voutilainen

Helsinki Institute of Physics, Helsinki, Finland
J. Härkönen, V. Karimäki, R. Kinnunen, T. Lampén, K. Lassila-Perini, S. Lehti, T. Lindén, P. Luukka, T. Mäenpää, T. Peltola, E. Tuominen, J. Tuominiemi, E. Tuovinen, L. Wendland

Lappeenranta University of Technology, Lappeenranta, Finland
J. Talvitie, T. Tuuva

IRFU, CEA, Université Paris-Saclay, Gif-sur-Yvette, France
M. Besancon, F. Couderc, M. Dejardin, D. Denegri, B. Fabbro, J.L. Faure, C. Favaro, F. Ferri, S. Ganjour, A. Givernaud, P. Gras, G. Hamel de Monchenault, P. Jarry, E. Locci, M. Machet, J. Malcles, J. Rander, A. Rosowsky, M. Titov, A. Zghiche

Laboratoire Leprince-Ringuet, Ecole Polytechnique, IN2P3-CNRS, Palaiseau, France
I. Antropov, S. Baffioni, F. Beaudette, P. Busson, L. Cadamuro, E. Chapon, C. Charlot, T. Dahms, O. Davignon, N. Filipovic, A. Florent, R. Granier de Cassagnac, S. Lisniak, L. Mastrolorenzo, P. Miné, I.N. Naranjo, M. Nguyen, C. Ochando, G. Ortona, P. Paganini, P. Pigard, S. Regnard, R. Salerno, J.B. Sauvan, Y. Sirois, T. Strebler, Y. Yilmaz, A. Zabi

Institut Pluridisciplinaire Hubert Curien, Université de Strasbourg, Université de Haute Alsace Mulhouse, CNRS/IN2P3, Strasbourg, France
J.-L. Agram[16], J. Andrea, A. Aubin, D. Bloch, J.-M. Brom, M. Buttignol, E.C. Chabert, N. Chanon, C. Collard, E. Conte[16], X. Coubez, J.-C. Fontaine[16], D. Gelé, U. Goerlach, C. Goetzmann, A.-C. Le Bihan, J.A. Merlin[2], K. Skovpen, P. Van Hove

Centre de Calcul de l'Institut National de Physique Nucleaire et de Physique des Particules, CNRS/IN2P3, Villeurbanne, France
S. Gadrat

Université de Lyon, Université Claude Bernard Lyon 1, CNRS-IN2P3, Institut de Physique Nucléaire de Lyon, Villeurbanne, France
S. Beauceron, C. Bernet, G. Boudoul, E. Bouvier, C.A. Carrillo Montoya, R. Chierici, D. Contardo, B. Courbon, P. Depasse, H. El Mamouni, J. Fan, J. Fay, S. Gascon, M. Gouzevitch, B. Ille, F. Lagarde, I.B. Laktineh, M. Lethuillier, L. Mirabito, A.L. Pequegnot, S. Perries, J.D. Ruiz Alvarez, D. Sabes, L. Sgandurra, V. Sordini, M. Vander Donckt, P. Verdier, S. Viret, H. Xiao

Georgian Technical University, Tbilisi, Georgia
T. Toriashvili[17]

Tbilisi State University, Tbilisi, Georgia
Z. Tsamalaidze[10]

RWTH Aachen University, I. Physikalisches Institut, Aachen, Germany
C. Autermann, S. Beranek, M. Edelhoff, L. Feld, A. Heister, M.K. Kiesel, K. Klein, M. Lipinski, A. Ostapchuk, M. Preuten, F. Raupach, S. Schael, J.F. Schulte, T. Verlage, H. Weber, B. Wittmer, V. Zhukov[6]

RWTH Aachen University, III. Physikalisches Institut A, Aachen, Germany
M. Ata, M. Brodski, E. Dietz-Laursonn, D. Duchardt, M. Endres, M. Erdmann, S. Erdweg, T. Esch, R. Fischer, A. Güth, T. Hebbeker, C. Heidemann, K. Hoepfner, D. Klingebiel, S. Knutzen, P. Kreuzer, M. Merschmeyer, A. Meyer, P. Millet, M. Olschewski, K. Padeken, P. Papacz, T. Pook, M. Radziej, H. Reithler, M. Rieger, F. Scheuch, L. Sonnenschein, D. Teyssier, S. Thüer

RWTH Aachen University, III. Physikalisches Institut B, Aachen, Germany
V. Cherepanov, Y. Erdogan, G. Flügge, H. Geenen, M. Geisler, F. Hoehle, B. Kargoll, T. Kress, Y. Kuessel, A. Künsken, J. Lingemann[2], A. Nehrkorn, A. Nowack, I.M. Nugent, C. Pistone, O. Pooth, A. Stahl

Deutsches Elektronen-Synchrotron, Hamburg, Germany
M. Aldaya Martin, I. Asin, N. Bartosik, O. Behnke, U. Behrens, A.J. Bell, K. Borras, A. Burgmeier, A. Cakir, L. Calligaris, A. Campbell, S. Choudhury, F. Costanza, C. Diez

Pardos, G. Dolinska, S. Dooling, T. Dorland, G. Eckerlin, D. Eckstein, T. Eichhorn, G. Flucke, E. Gallo[18], J. Garay Garcia, A. Geiser, A. Gizhko, P. Gunnellini, J. Hauk, M. Hempel[19], H. Jung, A. Kalogeropoulos, O. Karacheban[19], M. Kasemann, P. Katsas, J. Kieseler, C. Kleinwort, I. Korol, W. Lange, J. Leonard, K. Lipka, A. Lobanov, W. Lohmann[19], R. Mankel, I. Marfin[19], I.-A. Melzer-Pellmann, A.B. Meyer, G. Mittag, J. Mnich, A. Mussgiller, S. Naumann-Emme, A. Nayak, E. Ntomari, H. Perrey, D. Pitzl, R. Placakyte, A. Raspereza, B. Roland, M.Ö. Sahin, P. Saxena, T. Schoerner-Sadenius, M. Schröder, C. Seitz, S. Spannagel, K.D. Trippkewitz, R. Walsh, C. Wissing

University of Hamburg, Hamburg, Germany
V. Blobel, M. Centis Vignali, A.R. Draeger, J. Erfle, E. Garutti, K. Goebel, D. Gonzalez, M. Görner, J. Haller, M. Hoffmann, R.S. Höing, A. Junkes, R. Klanner, R. Kogler, T. Lapsien, T. Lenz, I. Marchesini, D. Marconi, M. Meyer, D. Nowatschin, J. Ott, F. Pantaleo[2], T. Peiffer, A. Perieanu, N. Pietsch, J. Poehlsen, D. Rathjens, C. Sander, H. Schettler, P. Schleper, E. Schlieckau, A. Schmidt, J. Schwandt, M. Seidel, V. Sola, H. Stadie, G. Steinbrück, H. Tholen, D. Troendle, E. Usai, L. Vanelderen, A. Vanhoefer, B. Vormwald

Institut für Experimentelle Kernphysik, Karlsruhe, Germany
M. Akbiyik, C. Barth, C. Baus, J. Berger, C. Böser, E. Butz, T. Chwalek, F. Colombo, W. De Boer, A. Descroix, A. Dierlamm, S. Fink, F. Frensch, M. Giffels, A. Gilbert, F. Hartmann[2], S.M. Heindl, U. Husemann, I. Katkov[6], A. Kornmayer[2], P. Lobelle Pardo, B. Maier, H. Mildner, M.U. Mozer, T. Müller, Th. Müller, M. Plagge, G. Quast, K. Rabbertz, S. Röcker, F. Roscher, H.J. Simonis, F.M. Stober, R. Ulrich, J. Wagner-Kuhr, S. Wayand, M. Weber, T. Weiler, C. Wöhrmann, R. Wolf

Institute of Nuclear and Particle Physics (INPP), NCSR Demokritos, Aghia Paraskevi, Greece
G. Anagnostou, G. Daskalakis, T. Geralis, V.A. Giakoumopoulou, A. Kyriakis, D. Loukas, A. Psallidas, I. Topsis-Giotis

National and Kapodistrian University of Athens, Athens, Greece
A. Agapitos, S. Kesisoglou, A. Panagiotou, N. Saoulidou, E. Tziaferi

University of Ioánnina, Ioánnina, Greece
I. Evangelou, G. Flouris, C. Foudas, P. Kokkas, N. Loukas, N. Manthos, I. Papadopoulos, E. Paradas, J. Strologas

Wigner Research Centre for Physics, Budapest, Hungary
G. Bencze, C. Hajdu, A. Hazi, P. Hidas, D. Horvath[20], F. Sikler, V. Veszpremi, G. Vesztergombi[21], A.J. Zsigmond

Institute of Nuclear Research ATOMKI, Debrecen, Hungary
N. Beni, S. Czellar, J. Karancsi[22], J. Molnar, Z. Szillasi

University of Debrecen, Debrecen, Hungary
M. Bartók[23], A. Makovec, P. Raics, Z.L. Trocsanyi, B. Ujvari

National Institute of Science Education and Research, Bhubaneswar, India
P. Mal, K. Mandal, N. Sahoo, S.K. Swain

Panjab University, Chandigarh, India
S. Bansal, S.B. Beri, V. Bhatnagar, R. Chawla, R. Gupta, U.Bhawandeep, A.K. Kalsi, A. Kaur, M. Kaur, R. Kumar, A. Mehta, M. Mittal, J.B. Singh, G. Walia

University of Delhi, Delhi, India
Ashok Kumar, A. Bhardwaj, B.C. Choudhary, R.B. Garg, A. Kumar, S. Malhotra, M. Naimuddin, N. Nishu, K. Ranjan, R. Sharma, V. Sharma

Saha Institute of Nuclear Physics, Kolkata, India
S. Banerjee, S. Bhattacharya, K. Chatterjee, S. Dey, S. Dutta, Sa. Jain, N. Majumdar, A. Modak, K. Mondal, S. Mukherjee, S. Mukhopadhyay, A. Roy, D. Roy, S. Roy Chowdhury, S. Sarkar, M. Sharan

Bhabha Atomic Research Centre, Mumbai, India
A. Abdulsalam, R. Chudasama, D. Dutta, V. Jha, V. Kumar, A.K. Mohanty[2], L.M. Pant, P. Shukla, A. Topkar

Tata Institute of Fundamental Research, Mumbai, India
T. Aziz, S. Banerjee, S. Bhowmik[24], R.M. Chatterjee, R.K. Dewanjee, S. Dugad, S. Ganguly, S. Ghosh, M. Guchait, A. Gurtu[25], G. Kole, S. Kumar, B. Mahakud, M. Maity[24], G. Majumder, K. Mazumdar, S. Mitra, G.B. Mohanty, B. Parida, T. Sarkar[24], K. Sudhakar, N. Sur, B. Sutar, N. Wickramage[26]

Indian Institute of Science Education and Research (IISER), Pune, India
S. Chauhan, S. Dube, S. Sharma

Institute for Research in Fundamental Sciences (IPM), Tehran, Iran
H. Bakhshiansohi, H. Behnamian, S.M. Etesami[27], A. Fahim[28], R. Goldouzian, M. Khakzad, M. Mohammadi Najafabadi, M. Naseri, S. Paktinat Mehdiabadi, F. Rezaei Hosseinabadi, B. Safarzadeh[29], M. Zeinali

University College Dublin, Dublin, Ireland
M. Felcini, M. Grunewald

INFN Sezione di Bari [a], Università di Bari [b], Politecnico di Bari [c], Bari, Italy
M. Abbrescia[a,b], C. Calabria[a,b], C. Caputo[a,b], A. Colaleo[a], D. Creanza[a,c], L. Cristella[a,b], N. De Filippis[a,c], M. De Palma[a,b], L. Fiore[a], G. Iaselli[a,c], G. Maggi[a,c], M. Maggi[a], G. Miniello[a,b], S. My[a,c], S. Nuzzo[a,b], A. Pompili[a,b], G. Pugliese[a,c], R. Radogna[a,b], A. Ranieri[a], G. Selvaggi[a,b], L. Silvestris[a,2], R. Venditti[a,b], P. Verwilligen[a]

INFN Sezione di Bologna [a], Università di Bologna [b], Bologna, Italy
G. Abbiendi[a], C. Battilana[2], A.C. Benvenuti[a], D. Bonacorsi[a,b], S. Braibant-Giacomelli[a,b], L. Brigliadori[a,b], R. Campanini[a,b], P. Capiluppi[a,b], A. Castro[a,b], F.R. Cavallo[a], S.S. Chhibra[a,b], G. Codispoti[a,b], M. Cuffiani[a,b], G.M. Dallavalle[a], F. Fabbri[a], A. Fanfani[a,b], D. Fasanella[a,b], P. Giacomelli[a], C. Grandi[a], L. Guiducci[a,b], S. Marcellini[a], G. Masetti[a], A. Montanari[a], F.L. Navarria[a,b], A. Perrotta[a], A.M. Rossi[a,b], T. Rovelli[a,b], G.P. Siroli[a,b], N. Tosi[a,b], R. Travaglini[a,b]

INFN Sezione di Catania [a], Università di Catania [b], Catania, Italy
G. Cappello[a], M. Chiorboli[a,b], S. Costa[a,b], F. Giordano[a,b], R. Potenza[a,b], A. Tricomi[a,b], C. Tuve[a,b]

INFN Sezione di Firenze [a], Università di Firenze [b], Firenze, Italy
G. Barbagli[a], V. Ciulli[a,b], C. Civinini[a], R. D'Alessandro[a,b], E. Focardi[a,b], S. Gonzi[a,b], V. Gori[a,b], P. Lenzi[a,b], M. Meschini[a], S. Paoletti[a], G. Sguazzoni[a], A. Tropiano[a,b], L. Viliani[a,b]

INFN Laboratori Nazionali di Frascati, Frascati, Italy
L. Benussi, S. Bianco, F. Fabbri, D. Piccolo, F. Primavera

INFN Sezione di Genova [a], Università di Genova [b], Genova, Italy
V. Calvelli[a,b], F. Ferro[a], M. Lo Vetere[a,b], M.R. Monge[a,b], E. Robutti[a], S. Tosi[a,b]

INFN Sezione di Milano-Bicocca [a], Università di Milano-Bicocca [b], Milano, Italy
L. Brianza, M.E. Dinardo[a,b], S. Fiorendi[a,b], S. Gennai[a], R. Gerosa[a,b], A. Ghezzi[a,b], P. Govoni[a,b], S. Malvezzi[a], R.A. Manzoni[a,b], B. Marzocchi[a,b,2], D. Menasce[a], L. Moroni[a], M. Paganoni[a,b], D. Pedrini[a], S. Ragazzi[a,b], N. Redaelli[a], T. Tabarelli de Fatis[a,b]

INFN Sezione di Napoli [a], Università di Napoli 'Federico II' [b], Napoli, Italy, Università della Basilicata [c], Potenza, Italy, Università G. Marconi [d], Roma, Italy
S. Buontempo[a], N. Cavallo[a,c], S. Di Guida[a,d,2], M. Esposito[a,b], F. Fabozzi[a,c], A.O.M. Iorio[a,b], G. Lanza[a], L. Lista[a], S. Meola[a,d,2], M. Merola[a], P. Paolucci[a,2], C. Sciacca[a,b], F. Thyssen

INFN Sezione di Padova [a], Università di Padova [b], Padova, Italy, Università di Trento [c], Trento, Italy
P. Azzi[a,2], N. Bacchetta[a], L. Benato[a,b], D. Bisello[a,b], A. Boletti[a,b], A. Branca[a,b], R. Carlin[a,b], P. Checchia[a], M. Dall'Osso[a,b,2], T. Dorigo[a], U. Dosselli[a], F. Gasparini[a,b], U. Gasparini[a,b], A. Gozzelino[a], K. Kanishchev[a,c], S. Lacaprara[a], M. Margoni[a,b], A.T. Meneguzzo[a,b], J. Pazzini[a,b], N. Pozzobon[a,b], P. Ronchese[a,b], F. Simonetto[a,b], E. Torassa[a], M. Tosi[a,b], S. Vanini[a,b], M. Zanetti, P. Zotto[a,b], A. Zucchetta[a,b,2], G. Zumerle[a,b]

INFN Sezione di Pavia [a], Università di Pavia [b], Pavia, Italy
A. Braghieri[a], A. Magnani[a], P. Montagna[a,b], S.P. Ratti[a,b], V. Re[a], C. Riccardi[a,b], P. Salvini[a], I. Vai[a], P. Vitulo[a,b]

INFN Sezione di Perugia [a], Università di Perugia [b], Perugia, Italy
L. Alunni Solestizi[a,b], M. Biasini[a,b], G.M. Bilei[a], D. Ciangottini[a,b,2], L. Fanò[a,b], P. Lariccia[a,b], G. Mantovani[a,b], M. Menichelli[a], A. Saha[a], A. Santocchia[a,b], A. Spiezia[a,b]

INFN Sezione di Pisa [a], Università di Pisa [b], Scuola Normale Superiore di Pisa [c], Pisa, Italy
K. Androsov[a,30], P. Azzurri[a], G. Bagliesi[a], J. Bernardini[a], T. Boccali[a], G. Broccolo[a,c], R. Castaldi[a], M.A. Ciocci[a,30], R. Dell'Orso[a], S. Donato[a,c,2], G. Fedi, L. Foà[a,c†], A. Giassi[a], M.T. Grippo[a,30], F. Ligabue[a,c], T. Lomtadze[a], L. Martini[a,b], A. Messineo[a,b], F. Palla[a], A. Rizzi[a,b], A. Savoy-Navarro[a,31], A.T. Serban[a], P. Spagnolo[a], P. Squillacioti[a,30], R. Tenchini[a], G. Tonelli[a,b], A. Venturi[a], P.G. Verdini[a]

INFN Sezione di Roma [a], Università di Roma [b], Roma, Italy
L. Barone[a,b], F. Cavallari[a], G. D'imperio[a,b,2], D. Del Re[a,b], M. Diemoz[a], S. Gelli[a,b], C. Jorda[a], E. Longo[a,b], F. Margaroli[a,b], P. Meridiani[a], G. Organtini[a,b], R. Paramatti[a], F. Preiato[a,b], S. Rahatlou[a,b], C. Rovelli[a], F. Santanastasio[a,b], P. Traczyk[a,b,2]

INFN Sezione di Torino [a], Università di Torino [b], Torino, Italy, Università del Piemonte Orientale [c], Novara, Italy
N. Amapane[a,b], R. Arcidiacono[a,c,2], S. Argiro[a,b], M. Arneodo[a,c], R. Bellan[a,b], C. Biino[a], N. Cartiglia[a], M. Costa[a,b], R. Covarelli[a,b], A. Degano[a,b], N. Demaria[a], L. Finco[a,b,2], C. Mariotti[a], S. Maselli[a], E. Migliore[a,b], V. Monaco[a,b], E. Monteil[a,b], M. Musich[a], M.M. Obertino[a,b], L. Pacher[a,b], N. Pastrone[a], M. Pelliccioni[a], G.L. Pinna Angioni[a,b], F. Ravera[a,b], A. Romero[a,b], M. Ruspa[a,c], R. Sacchi[a,b], A. Solano[a,b], A. Staiano[a], U. Tamponi[a], L. Visca[a,b]

INFN Sezione di Trieste [a], Università di Trieste [b], Trieste, Italy
S. Belforte[a], V. Candelise[a,b,2], M. Casarsa[a], F. Cossutti[a], G. Della Ricca[a,b], B. Gobbo[a], C. La Licata[a,b], M. Marone[a,b], A. Schizzi[a,b], A. Zanetti[a]

Kangwon National University, Chunchon, Korea
A. Kropivnitskaya, S.K. Nam

Kyungpook National University, Daegu, Korea
D.H. Kim, G.N. Kim, M.S. Kim, D.J. Kong, S. Lee, Y.D. Oh, A. Sakharov, D.C. Son

Chonbuk National University, Jeonju, Korea
J.A. Brochero Cifuentes, H. Kim, T.J. Kim[32], M.S. Ryu

Chonnam National University, Institute for Universe and Elementary Particles, Kwangju, Korea
S. Song

Korea University, Seoul, Korea
S. Choi, Y. Go, D. Gyun, B. Hong, M. Jo, H. Kim, Y. Kim, B. Lee, K. Lee, K.S. Lee, S. Lee, S.K. Park, Y. Roh

Seoul National University, Seoul, Korea
H.D. Yoo

University of Seoul, Seoul, Korea
M. Choi, H. Kim, J.H. Kim, J.S.H. Lee, I.C. Park, G. Ryu

Sungkyunkwan University, Suwon, Korea
Y. Choi, Y.K. Choi, J. Goh, D. Kim, E. Kwon, J. Lee, I. Yu

Vilnius University, Vilnius, Lithuania
A. Juodagalvis, J. Vaitkus

National Centre for Particle Physics, Universiti Malaya, Kuala Lumpur, Malaysia
I. Ahmed, Z.A. Ibrahim, J.R. Komaragiri, M.A.B. Md Ali[33], F. Mohamad Idris[34], W.A.T. Wan Abdullah, M.N. Yusli

Centro de Investigacion y de Estudios Avanzados del IPN, Mexico City, Mexico
E. Casimiro Linares, H. Castilla-Valdez, E. De La Cruz-Burelo, I. Heredia-de La Cruz[35], A. Hernandez-Almada, R. Lopez-Fernandez, A. Sanchez-Hernandez

Universidad Iberoamericana, Mexico City, Mexico
S. Carrillo Moreno, F. Vazquez Valencia

Benemerita Universidad Autonoma de Puebla, Puebla, Mexico
I. Pedraza, H.A. Salazar Ibarguen

Universidad Autónoma de San Luis Potosí, San Luis Potosí, Mexico
A. Morelos Pineda

University of Auckland, Auckland, New Zealand
D. Krofcheck

University of Canterbury, Christchurch, New Zealand
P.H. Butler

National Centre for Physics, Quaid-I-Azam University, Islamabad, Pakistan
A. Ahmad, M. Ahmad, Q. Hassan, H.R. Hoorani, W.A. Khan, T. Khurshid, M. Shoaib

National Centre for Nuclear Research, Swierk, Poland
H. Bialkowska, M. Bluj, B. Boimska, T. Frueboes, M. Górski, M. Kazana, K. Nawrocki, K. Romanowska-Rybinska, M. Szleper, P. Zalewski

Institute of Experimental Physics, Faculty of Physics, University of Warsaw, Warsaw, Poland
G. Brona, K. Bunkowski, K. Doroba, A. Kalinowski, M. Konecki, J. Krolikowski, M. Misiura, M. Olszewski, M. Walczak

Laboratório de Instrumentação e Física Experimental de Partículas, Lisboa, Portugal
P. Bargassa, C. Beirão Da Cruz E Silva, A. Di Francesco, P. Faccioli, P.G. Ferreira Parracho, M. Gallinaro, N. Leonardo, L. Lloret Iglesias, F. Nguyen, J. Rodrigues Antunes, J. Seixas, O. Toldaiev, D. Vadruccio, J. Varela, P. Vischia

Joint Institute for Nuclear Research, Dubna, Russia
S. Afanasiev, P. Bunin, M. Gavrilenko, I. Golutvin, I. Gorbunov, A. Kamenev, V. Karjavin, V. Konoplyanikov, A. Lanev, A. Malakhov, V. Matveev[36], P. Moisenz, V. Palichik, V. Perelygin, S. Shmatov, S. Shulha, N. Skatchkov, V. Smirnov, A. Zarubin

Petersburg Nuclear Physics Institute, Gatchina (St. Petersburg), Russia
V. Golovtsov, Y. Ivanov, V. Kim[37], E. Kuznetsova, P. Levchenko, V. Murzin, V. Oreshkin, I. Smirnov, V. Sulimov, L. Uvarov, S. Vavilov, A. Vorobyev

Institute for Nuclear Research, Moscow, Russia
Yu. Andreev, A. Dermenev, S. Gninenko, N. Golubev, A. Karneyeu, M. Kirsanov, N. Krasnikov, A. Pashenkov, D. Tlisov, A. Toropin

Institute for Theoretical and Experimental Physics, Moscow, Russia
V. Epshteyn, V. Gavrilov, N. Lychkovskaya, V. Popov, I. Pozdnyakov, G. Safronov, A. Spiridonov, E. Vlasov, A. Zhokin

National Research Nuclear University 'Moscow Engineering Physics Institute' (MEPhI), Moscow, Russia
A. Bylinkin

P.N. Lebedev Physical Institute, Moscow, Russia
V. Andreev, M. Azarkin[38], I. Dremin[38], M. Kirakosyan, A. Leonidov[38], G. Mesyats, S.V. Rusakov, A. Vinogradov

Skobeltsyn Institute of Nuclear Physics, Lomonosov Moscow State University, Moscow, Russia
A. Baskakov, A. Belyaev, E. Boos, V. Bunichev, M. Dubinin[39], L. Dudko, A. Gribushin, V. Klyukhin, N. Korneeva, I. Lokhtin, I. Myagkov, S. Obraztsov, M. Perfilov, V. Savrin, A. Snigirev

State Research Center of Russian Federation, Institute for High Energy Physics, Protvino, Russia
I. Azhgirey, I. Bayshev, S. Bitioukov, V. Kachanov, A. Kalinin, D. Konstantinov, V. Krychkine, V. Petrov, R. Ryutin, A. Sobol, L. Tourtchanovitch, S. Troshin, N. Tyurin, A. Uzunian, A. Volkov

University of Belgrade, Faculty of Physics and Vinca Institute of Nuclear Sciences, Belgrade, Serbia
P. Adzic[40], M. Ekmedzic, J. Milosevic, V. Rekovic

Centro de Investigaciones Energéticas Medioambientales y Tecnológicas (CIEMAT), Madrid, Spain
J. Alcaraz Maestre, E. Calvo, M. Cerrada, M. Chamizo Llatas, N. Colino, B. De La Cruz, A. Delgado Peris, D. Domínguez Vázquez, A. Escalante Del Valle, C. Fernandez Bedoya, J.P. Fernández Ramos, J. Flix, M.C. Fouz, P. Garcia-Abia, O. Gonzalez Lopez, S. Goy Lopez,

J.M. Hernandez, M.I. Josa, E. Navarro De Martino, A. Pérez-Calero Yzquierdo, J. Puerta Pelayo, A. Quintario Olmeda, I. Redondo, L. Romero, M.S. Soares

Universidad Autónoma de Madrid, Madrid, Spain
C. Albajar, J.F. de Trocóniz, M. Missiroli, D. Moran

Universidad de Oviedo, Oviedo, Spain
H. Brun, J. Cuevas, J. Fernandez Menendez, S. Folgueras, I. Gonzalez Caballero, E. Palencia Cortezon, J.M. Vizan Garcia

Instituto de Física de Cantabria (IFCA), CSIC-Universidad de Cantabria, Santander, Spain
I.J. Cabrillo, A. Calderon, J.R. Castiñeiras De Saa, P. De Castro Manzano, J. Duarte Campderros, M. Fernandez, J. Garcia-Ferrero, G. Gomez, A. Lopez Virto, J. Marco, R. Marco, C. Martinez Rivero, F. Matorras, F.J. Munoz Sanchez, J. Piedra Gomez, T. Rodrigo, A.Y. Rodríguez-Marrero, A. Ruiz-Jimeno, L. Scodellaro, I. Vila, R. Vilar Cortabitarte

CERN, European Organization for Nuclear Research, Geneva, Switzerland
D. Abbaneo, E. Auffray, G. Auzinger, M. Bachtis, P. Baillon, A.H. Ball, D. Barney, A. Benaglia, J. Bendavid, L. Benhabib, J.F. Benitez, G.M. Berruti, P. Bloch, A. Bocci, A. Bonato, C. Botta, H. Breuker, T. Camporesi, G. Cerminara, S. Colafranceschi[41], M. D'Alfonso, D. d'Enterria, A. Dabrowski, V. Daponte, A. David, M. De Gruttola, F. De Guio, A. De Roeck, S. De Visscher, E. Di Marco, M. Dobson, M. Dordevic, B. Dorney, T. du Pree, M. Dünser, N. Dupont, A. Elliott-Peisert, G. Franzoni, W. Funk, D. Gigi, K. Gill, D. Giordano, M. Girone, F. Glege, R. Guida, S. Gundacker, M. Guthoff, J. Hammer, P. Harris, J. Hegeman, V. Innocente, P. Janot, H. Kirschenmann, M.J. Kortelainen, K. Kousouris, K. Krajczar, P. Lecoq, C. Lourenço, M.T. Lucchini, N. Magini, L. Malgeri, M. Mannelli, A. Martelli, L. Masetti, F. Meijers, S. Mersi, E. Meschi, F. Moortgat, S. Morovic, M. Mulders, M.V. Nemallapudi, H. Neugebauer, S. Orfanelli[42], L. Orsini, L. Pape, E. Perez, M. Peruzzi, A. Petrilli, G. Petrucciani, A. Pfeiffer, D. Piparo, A. Racz, G. Rolandi[43], M. Rovere, M. Ruan, H. Sakulin, C. Schäfer, C. Schwick, A. Sharma, P. Silva, M. Simon, P. Sphicas[44], D. Spiga, J. Steggemann, B. Stieger, M. Stoye, Y. Takahashi, D. Treille, A. Triossi, A. Tsirou, G.I. Veres[21], N. Wardle, H.K. Wöhri, A. Zagozdzinska[45], W.D. Zeuner

Paul Scherrer Institut, Villigen, Switzerland
W. Bertl, K. Deiters, W. Erdmann, R. Horisberger, Q. Ingram, H.C. Kaestli, D. Kotlinski, U. Langenegger, D. Renker, T. Rohe

Institute for Particle Physics, ETH Zurich, Zurich, Switzerland
F. Bachmair, L. Bäni, L. Bianchini, M.A. Buchmann, B. Casal, G. Dissertori, M. Dittmar, M. Donegà, P. Eller, C. Grab, C. Heidegger, D. Hits, J. Hoss, G. Kasieczka, W. Lustermann, B. Mangano, M. Marionneau, P. Martinez Ruiz del Arbol, M. Masciovecchio, D. Meister, F. Micheli, P. Musella, F. Nessi-Tedaldi, F. Pandolfi, J. Pata, F. Pauss, L. Perrozzi, M. Quittnat, M. Rossini, A. Starodumov[46], M. Takahashi, V.R. Tavolaro, K. Theofilatos, R. Wallny

Universität Zürich, Zurich, Switzerland
T.K. Aarrestad, C. Amsler[47], L. Caminada, M.F. Canelli, V. Chiochia, A. De Cosa, C. Galloni, A. Hinzmann, T. Hreus, B. Kilminster, C. Lange, J. Ngadiuba, D. Pinna, P. Robmann, F.J. Ronga, D. Salerno, Y. Yang

National Central University, Chung-Li, Taiwan
M. Cardaci, K.H. Chen, T.H. Doan, Sh. Jain, R. Khurana, M. Konyushikhin, C.M. Kuo, W. Lin, Y.J. Lu, S.S. Yu

National Taiwan University (NTU), Taipei, Taiwan
Arun Kumar, R. Bartek, P. Chang, Y.H. Chang, Y.W. Chang, Y. Chao, K.F. Chen, P.H. Chen, C. Dietz, F. Fiori, U. Grundler, W.-S. Hou, Y. Hsiung, Y.F. Liu, R.-S. Lu, M. Miñano Moya, E. Petrakou, J.F. Tsai, Y.M. Tzeng

Chulalongkorn University, Faculty of Science, Department of Physics, Bangkok, Thailand
B. Asavapibhop, K. Kovitanggoon, G. Singh, N. Srimanobhas, N. Suwonjandee

Cukurova University, Adana, Turkey
A. Adiguzel, S. Cerci[48], Z.S. Demiroglu, C. Dozen, I. Dumanoglu, S. Girgis, G. Gokbulut, Y. Guler, E. Gurpinar, I. Hos, E.E. Kangal[49], A. Kayis Topaksu, G. Onengut[50], K. Ozdemir[51], S. Ozturk[52], B. Tali[48], H. Topakli[52], M. Vergili, C. Zorbilmez

Middle East Technical University, Physics Department, Ankara, Turkey
I.V. Akin, B. Bilin, S. Bilmis, B. Isildak[53], G. Karapinar[54], M. Yalvac, M. Zeyrek

Bogazici University, Istanbul, Turkey
E.A. Albayrak[55], E. Gülmez, M. Kaya[56], O. Kaya[57], T. Yetkin[58]

Istanbul Technical University, Istanbul, Turkey
K. Cankocak, S. Sen[59], F.I. Vardarlı

Institute for Scintillation Materials of National Academy of Science of Ukraine, Kharkov, Ukraine
B. Grynyov

National Scientific Center, Kharkov Institute of Physics and Technology, Kharkov, Ukraine
L. Levchuk, P. Sorokin

University of Bristol, Bristol, United Kingdom
R. Aggleton, F. Ball, L. Beck, J.J. Brooke, E. Clement, D. Cussans, H. Flacher, J. Goldstein, M. Grimes, G.P. Heath, H.F. Heath, J. Jacob, L. Kreczko, C. Lucas, Z. Meng, D.M. Newbold[60], S. Paramesvaran, A. Poll, T. Sakuma, S. Seif El Nasr-storey, S. Senkin, D. Smith, V.J. Smith

Rutherford Appleton Laboratory, Didcot, United Kingdom
K.W. Bell, A. Belyaev[61], C. Brew, R.M. Brown, D. Cieri, D.J.A. Cockerill, J.A. Coughlan, K. Harder, S. Harper, E. Olaiya, D. Petyt, C.H. Shepherd-Themistocleous, A. Thea, L. Thomas, I.R. Tomalin, T. Williams, W.J. Womersley, S.D. Worm

Imperial College, London, United Kingdom
M. Baber, R. Bainbridge, O. Buchmuller, A. Bundock, D. Burton, S. Casasso, M. Citron, D. Colling, L. Corpe, N. Cripps, P. Dauncey, G. Davies, A. De Wit, M. Della Negra, P. Dunne, A. Elwood, W. Ferguson, J. Fulcher, D. Futyan, G. Hall, G. Iles, M. Kenzie, R. Lane, R. Lucas[60], L. Lyons, A.-M. Magnan, S. Malik, J. Nash, A. Nikitenko[46], J. Pela, M. Pesaresi, K. Petridis, D.M. Raymond, A. Richards, A. Rose, C. Seez, A. Tapper, K. Uchida, M. Vazquez Acosta[62], T. Virdee, S.C. Zenz

Brunel University, Uxbridge, United Kingdom
J.E. Cole, P.R. Hobson, A. Khan, P. Kyberd, D. Leggat, D. Leslie, I.D. Reid, P. Symonds, L. Teodorescu, M. Turner

Baylor University, Waco, USA
A. Borzou, K. Call, J. Dittmann, K. Hatakeyama, A. Kasmi, H. Liu, N. Pastika

The University of Alabama, Tuscaloosa, USA
O. Charaf, S.I. Cooper, C. Henderson, P. Rumerio

Boston University, Boston, USA
A. Avetisyan, T. Bose, C. Fantasia, D. Gastler, P. Lawson, D. Rankin, C. Richardson, J. Rohlf, J. St. John, L. Sulak, D. Zou

Brown University, Providence, USA
J. Alimena, E. Berry, S. Bhattacharya, D. Cutts, N. Dhingra, A. Ferapontov, A. Garabedian, J. Hakala, U. Heintz, E. Laird, G. Landsberg, Z. Mao, M. Narain, S. Piperov, S. Sagir, T. Sinthuprasith, R. Syarif

University of California, Davis, Davis, USA
R. Breedon, G. Breto, M. Calderon De La Barca Sanchez, S. Chauhan, M. Chertok, J. Conway, R. Conway, P.T. Cox, R. Erbacher, M. Gardner, W. Ko, R. Lander, M. Mulhearn, D. Pellett, J. Pilot, F. Ricci-Tam, S. Shalhout, J. Smith, M. Squires, D. Stolp, M. Tripathi, S. Wilbur, R. Yohay

University of California, Los Angeles, USA
R. Cousins, P. Everaerts, C. Farrell, J. Hauser, M. Ignatenko, D. Saltzberg, E. Takasugi, V. Valuev, M. Weber

University of California, Riverside, Riverside, USA
K. Burt, R. Clare, J. Ellison, J.W. Gary, G. Hanson, J. Heilman, M. Ivova PANEVA, P. Jandir, E. Kennedy, F. Lacroix, O.R. Long, A. Luthra, M. Malberti, M. Olmedo Negrete, A. Shrinivas, H. Wei, S. Wimpenny

University of California, San Diego, La Jolla, USA
J.G. Branson, G.B. Cerati, S. Cittolin, R.T. D'Agnolo, A. Holzner, R. Kelley, D. Klein, J. Letts, I. Macneill, D. Olivito, S. Padhi, M. Pieri, M. Sani, V. Sharma, S. Simon, M. Tadel, A. Vartak, S. Wasserbaech[63], C. Welke, F. Würthwein, A. Yagil, G. Zevi Della Porta

University of California, Santa Barbara, Santa Barbara, USA
D. Barge, J. Bradmiller-Feld, C. Campagnari, A. Dishaw, V. Dutta, K. Flowers, M. Franco Sevilla, P. Geffert, C. George, F. Golf, L. Gouskos, J. Gran, J. Incandela, C. Justus, N. Mccoll, S.D. Mullin, J. Richman, D. Stuart, I. Suarez, W. To, C. West, J. Yoo

California Institute of Technology, Pasadena, USA
D. Anderson, A. Apresyan, A. Bornheim, J. Bunn, Y. Chen, J. Duarte, A. Mott, H.B. Newman, C. Pena, M. Pierini, M. Spiropulu, J.R. Vlimant, S. Xie, R.Y. Zhu

Carnegie Mellon University, Pittsburgh, USA
V. Azzolini, A. Calamba, B. Carlson, T. Ferguson, M. Paulini, J. Russ, M. Sun, H. Vogel, I. Vorobiev

University of Colorado Boulder, Boulder, USA
J.P. Cumalat, W.T. Ford, A. Gaz, F. Jensen, A. Johnson, M. Krohn, T. Mulholland, U. Nauenberg, K. Stenson, S.R. Wagner

Cornell University, Ithaca, USA
J. Alexander, A. Chatterjee, J. Chaves, J. Chu, S. Dittmer, N. Eggert, N. Mirman, G. Nicolas Kaufman, J.R. Patterson, A. Rinkevicius, A. Ryd, L. Skinnari, L. Soffi, W. Sun, S.M. Tan, W.D. Teo, J. Thom, J. Thompson, J. Tucker, Y. Weng, P. Wittich

Fermi National Accelerator Laboratory, Batavia, USA
S. Abdullin, M. Albrow, J. Anderson, G. Apollinari, L.A.T. Bauerdick, A. Beretvas, J. Berryhill, P.C. Bhat, G. Bolla, K. Burkett, J.N. Butler, H.W.K. Cheung, F. Chlebana, S. Cihangir, V.D. Elvira, I. Fisk, J. Freeman, E. Gottschalk, L. Gray, D. Green, S. Grünendahl, O. Gutsche, J. Hanlon, D. Hare, R.M. Harris, J. Hirschauer, B. Hooberman, Z. Hu, S. Jindariani, M. Johnson, U. Joshi,

A.W. Jung, B. Klima, B. Kreis, S. Kwan[†], S. Lammel, J. Linacre, D. Lincoln, R. Lipton, T. Liu, R. Lopes De Sá, J. Lykken, K. Maeshima, J.M. Marraffino, V.I. Martinez Outschoorn, S. Maruyama, D. Mason, P. McBride, P. Merkel, K. Mishra, S. Mrenna, S. Nahn, C. Newman-Holmes, V. O'Dell, K. Pedro, O. Prokofyev, G. Rakness, E. Sexton-Kennedy, A. Soha, W.J. Spalding, L. Spiegel, L. Taylor, S. Tkaczyk, N.V. Tran, L. Uplegger, E.W. Vaandering, C. Vernieri, M. Verzocchi, R. Vidal, H.A. Weber, A. Whitbeck, F. Yang

University of Florida, Gainesville, USA
D. Acosta, P. Avery, P. Bortignon, D. Bourilkov, A. Carnes, M. Carver, D. Curry, S. Das, G.P. Di Giovanni, R.D. Field, I.K. Furic, J. Hugon, J. Konigsberg, A. Korytov, J.F. Low, P. Ma, K. Matchev, H. Mei, P. Milenovic[64], G. Mitselmakher, D. Rank, R. Rossin, L. Shchutska, M. Snowball, D. Sperka, J. Wang, S. Wang, J. Yelton

Florida International University, Miami, USA
S. Hewamanage, S. Linn, P. Markowitz, G. Martinez, J.L. Rodriguez

Florida State University, Tallahassee, USA
A. Ackert, J.R. Adams, T. Adams, A. Askew, J. Bochenek, B. Diamond, J. Haas, S. Hagopian, V. Hagopian, K.F. Johnson, A. Khatiwada, H. Prosper, V. Veeraraghavan, M. Weinberg

Florida Institute of Technology, Melbourne, USA
M.M. Baarmand, V. Bhopatkar, M. Hohlmann, H. Kalakhety, D. Noonan, T. Roy, F. Yumiceva

University of Illinois at Chicago (UIC), Chicago, USA
M.R. Adams, L. Apanasevich, D. Berry, R.R. Betts, I. Bucinskaite, R. Cavanaugh, O. Evdokimov, L. Gauthier, C.E. Gerber, D.J. Hofman, P. Kurt, C. O'Brien, I.D. Sandoval Gonzalez, C. Silkworth, P. Turner, N. Varelas, Z. Wu, M. Zakaria

The University of Iowa, Iowa City, USA
B. Bilki[65], W. Clarida, K. Dilsiz, S. Durgut, R.P. Gandrajula, M. Haytmyradov, V. Khristenko, J.-P. Merlo, H. Mermerkaya[66], A. Mestvirishvili, A. Moeller, J. Nachtman, H. Ogul, Y. Onel, F. Ozok[55], A. Penzo, C. Snyder, P. Tan, E. Tiras, J. Wetzel, K. Yi

Johns Hopkins University, Baltimore, USA
I. Anderson, B.A. Barnett, B. Blumenfeld, D. Fehling, L. Feng, A.V. Gritsan, P. Maksimovic, C. Martin, M. Osherson, M. Swartz, M. Xiao, Y. Xin, C. You

The University of Kansas, Lawrence, USA
P. Baringer, A. Bean, G. Benelli, C. Bruner, R.P. Kenny III, D. Majumder, M. Malek, M. Murray, S. Sanders, R. Stringer, Q. Wang, J.S. Wood

Kansas State University, Manhattan, USA
A. Ivanov, K. Kaadze, S. Khalil, M. Makouski, Y. Maravin, A. Mohammadi, L.K. Saini, N. Skhirtladze, S. Toda

Lawrence Livermore National Laboratory, Livermore, USA
D. Lange, F. Rebassoo, D. Wright

University of Maryland, College Park, USA
C. Anelli, A. Baden, O. Baron, A. Belloni, B. Calvert, S.C. Eno, C. Ferraioli, J.A. Gomez, N.J. Hadley, S. Jabeen, R.G. Kellogg, T. Kolberg, J. Kunkle, Y. Lu, A.C. Mignerey, Y.H. Shin, A. Skuja, M.B. Tonjes, S.C. Tonwar

Massachusetts Institute of Technology, Cambridge, USA
A. Apyan, R. Barbieri, A. Baty, K. Bierwagen, S. Brandt, W. Busza, I.A. Cali, Z. Demiragli,

L. Di Matteo, G. Gomez Ceballos, M. Goncharov, D. Gulhan, Y. Iiyama, G.M. Innocenti, M. Klute, D. Kovalskyi, Y.S. Lai, Y.-J. Lee, A. Levin, P.D. Luckey, A.C. Marini, C. Mcginn, C. Mironov, X. Niu, C. Paus, D. Ralph, C. Roland, G. Roland, J. Salfeld-Nebgen, G.S.F. Stephans, K. Sumorok, M. Varma, D. Velicanu, J. Veverka, J. Wang, T.W. Wang, B. Wyslouch, M. Yang, V. Zhukova

University of Minnesota, Minneapolis, USA
B. Dahmes, A. Finkel, A. Gude, P. Hansen, S. Kalafut, S.C. Kao, K. Klapoetke, Y. Kubota, Z. Lesko, J. Mans, S. Nourbakhsh, N. Ruckstuhl, R. Rusack, N. Tambe, J. Turkewitz

University of Mississippi, Oxford, USA
J.G. Acosta, S. Oliveros

University of Nebraska-Lincoln, Lincoln, USA
E. Avdeeva, K. Bloom, S. Bose, D.R. Claes, A. Dominguez, C. Fangmeier, R. Gonzalez Suarez, R. Kamalieddin, J. Keller, D. Knowlton, I. Kravchenko, J. Lazo-Flores, F. Meier, J. Monroy, F. Ratnikov, J.E. Siado, G.R. Snow

State University of New York at Buffalo, Buffalo, USA
M. Alyari, J. Dolen, J. George, A. Godshalk, C. Harrington, I. Iashvili, J. Kaisen, A. Kharchilava, A. Kumar, S. Rappoccio

Northeastern University, Boston, USA
G. Alverson, E. Barberis, D. Baumgartel, M. Chasco, A. Hortiangtham, A. Massironi, D.M. Morse, D. Nash, T. Orimoto, R. Teixeira De Lima, D. Trocino, R.-J. Wang, D. Wood, J. Zhang

Northwestern University, Evanston, USA
K.A. Hahn, A. Kubik, N. Mucia, N. Odell, B. Pollack, A. Pozdnyakov, M. Schmitt, S. Stoynev, K. Sung, M. Trovato, M. Velasco

University of Notre Dame, Notre Dame, USA
A. Brinkerhoff, N. Dev, M. Hildreth, C. Jessop, D.J. Karmgard, N. Kellams, K. Lannon, S. Lynch, N. Marinelli, F. Meng, C. Mueller, Y. Musienko[36], T. Pearson, M. Planer, A. Reinsvold, R. Ruchti, G. Smith, S. Taroni, N. Valls, M. Wayne, M. Wolf, A. Woodard

The Ohio State University, Columbus, USA
L. Antonelli, J. Brinson, B. Bylsma, L.S. Durkin, S. Flowers, A. Hart, C. Hill, R. Hughes, W. Ji, K. Kotov, T.Y. Ling, B. Liu, W. Luo, D. Puigh, M. Rodenburg, B.L. Winer, H.W. Wulsin

Princeton University, Princeton, USA
O. Driga, P. Elmer, J. Hardenbrook, P. Hebda, S.A. Koay, P. Lujan, D. Marlow, T. Medvedeva, M. Mooney, J. Olsen, C. Palmer, P. Piroué, X. Quan, H. Saka, D. Stickland, C. Tully, J.S. Werner, A. Zuranski

University of Puerto Rico, Mayaguez, USA
S. Malik

Purdue University, West Lafayette, USA
V.E. Barnes, D. Benedetti, D. Bortoletto, L. Gutay, M.K. Jha, M. Jones, K. Jung, M. Kress, D.H. Miller, N. Neumeister, B.C. Radburn-Smith, X. Shi, I. Shipsey, D. Silvers, J. Sun, A. Svyatkovskiy, F. Wang, W. Xie, L. Xu

Purdue University Calumet, Hammond, USA
N. Parashar, J. Stupak

Rice University, Houston, USA
A. Adair, B. Akgun, Z. Chen, K.M. Ecklund, F.J.M. Geurts, M. Guilbaud, W. Li, B. Michlin, M. Northup, B.P. Padley, R. Redjimi, J. Roberts, J. Rorie, Z. Tu, J. Zabel

University of Rochester, Rochester, USA
B. Betchart, A. Bodek, P. de Barbaro, R. Demina, Y. Eshaq, T. Ferbel, M. Galanti, A. Garcia-Bellido, P. Goldenzweig, J. Han, A. Harel, O. Hindrichs, A. Khukhunaishvili, G. Petrillo, M. Verzetti

The Rockefeller University, New York, USA
L. Demortier

Rutgers, The State University of New Jersey, Piscataway, USA
S. Arora, A. Barker, J.P. Chou, C. Contreras-Campana, E. Contreras-Campana, D. Duggan, D. Ferencek, Y. Gershtein, R. Gray, E. Halkiadakis, D. Hidas, E. Hughes, S. Kaplan, R. Kunnawalkam Elayavalli, A. Lath, K. Nash, S. Panwalkar, M. Park, S. Salur, S. Schnetzer, D. Sheffield, S. Somalwar, R. Stone, S. Thomas, P. Thomassen, M. Walker

University of Tennessee, Knoxville, USA
M. Foerster, G. Riley, K. Rose, S. Spanier, A. York

Texas A&M University, College Station, USA
O. Bouhali[67], A. Castaneda Hernandez, M. Dalchenko, M. De Mattia, A. Delgado, S. Dildick, R. Eusebi, W. Flanagan, J. Gilmore, T. Kamon[68], V. Krutelyov, R. Montalvo, R. Mueller, I. Osipenkov, Y. Pakhotin, R. Patel, A. Perloff, J. Roe, A. Rose, A. Safonov, A. Tatarinov, K.A. Ulmer[2]

Texas Tech University, Lubbock, USA
N. Akchurin, C. Cowden, J. Damgov, C. Dragoiu, P.R. Dudero, J. Faulkner, S. Kunori, K. Lamichhane, S.W. Lee, T. Libeiro, S. Undleeb, I. Volobouev

Vanderbilt University, Nashville, USA
E. Appelt, A.G. Delannoy, S. Greene, A. Gurrola, R. Janjam, W. Johns, C. Maguire, Y. Mao, A. Melo, H. Ni, P. Sheldon, B. Snook, S. Tuo, J. Velkovska, Q. Xu

University of Virginia, Charlottesville, USA
M.W. Arenton, S. Boutle, B. Cox, B. Francis, J. Goodell, R. Hirosky, A. Ledovskoy, H. Li, C. Lin, C. Neu, E. Wolfe, J. Wood, F. Xia

Wayne State University, Detroit, USA
C. Clarke, R. Harr, P.E. Karchin, C. Kottachchi Kankanamge Don, P. Lamichhane, J. Sturdy

University of Wisconsin - Madison, Madison, WI, USA
D.A. Belknap, D. Carlsmith, M. Cepeda, A. Christian, S. Dasu, L. Dodd, S. Duric, E. Friis, B. Gomber, R. Hall-Wilton, M. Herndon, A. Hervé, P. Klabbers, A. Lanaro, A. Levine, K. Long, R. Loveless, A. Mohapatra, I. Ojalvo, T. Perry, G.A. Pierro, G. Polese, I. Ross, T. Ruggles, T. Sarangi, A. Savin, A. Sharma, N. Smith, W.H. Smith, D. Taylor, N. Woods

†: Deceased
1: Also at Vienna University of Technology, Vienna, Austria
2: Also at CERN, European Organization for Nuclear Research, Geneva, Switzerland
3: Also at State Key Laboratory of Nuclear Physics and Technology, Peking University, Beijing, China
4: Also at Institut Pluridisciplinaire Hubert Curien, Université de Strasbourg, Université de Haute Alsace Mulhouse, CNRS/IN2P3, Strasbourg, France

5: Also at National Institute of Chemical Physics and Biophysics, Tallinn, Estonia
6: Also at Skobeltsyn Institute of Nuclear Physics, Lomonosov Moscow State University, Moscow, Russia
7: Also at Universidade Estadual de Campinas, Campinas, Brazil
8: Also at Centre National de la Recherche Scientifique (CNRS) - IN2P3, Paris, France
9: Also at Laboratoire Leprince-Ringuet, Ecole Polytechnique, IN2P3-CNRS, Palaiseau, France
10: Also at Joint Institute for Nuclear Research, Dubna, Russia
11: Also at Beni-Suef University, Bani Sweif, Egypt
12: Now at British University in Egypt, Cairo, Egypt
13: Now at Ain Shams University, Cairo, Egypt
14: Also at Zewail City of Science and Technology, Zewail, Egypt
15: Now at Fayoum University, El-Fayoum, Egypt
16: Also at Université de Haute Alsace, Mulhouse, France
17: Also at Tbilisi State University, Tbilisi, Georgia
18: Also at University of Hamburg, Hamburg, Germany
19: Also at Brandenburg University of Technology, Cottbus, Germany
20: Also at Institute of Nuclear Research ATOMKI, Debrecen, Hungary
21: Also at Eötvös Loránd University, Budapest, Hungary
22: Also at University of Debrecen, Debrecen, Hungary
23: Also at Wigner Research Centre for Physics, Budapest, Hungary
24: Also at University of Visva-Bharati, Santiniketan, India
25: Now at King Abdulaziz University, Jeddah, Saudi Arabia
26: Also at University of Ruhuna, Matara, Sri Lanka
27: Also at Isfahan University of Technology, Isfahan, Iran
28: Also at University of Tehran, Department of Engineering Science, Tehran, Iran
29: Also at Plasma Physics Research Center, Science and Research Branch, Islamic Azad University, Tehran, Iran
30: Also at Università degli Studi di Siena, Siena, Italy
31: Also at Purdue University, West Lafayette, USA
32: Now at Hanyang University, Seoul, Korea
33: Also at International Islamic University of Malaysia, Kuala Lumpur, Malaysia
34: Also at Malaysian Nuclear Agency, MOSTI, Kajang, Malaysia
35: Also at Consejo Nacional de Ciencia y Tecnología, Mexico city, Mexico
36: Also at Institute for Nuclear Research, Moscow, Russia
37: Also at St. Petersburg State Polytechnical University, St. Petersburg, Russia
38: Also at National Research Nuclear University 'Moscow Engineering Physics Institute' (MEPhI), Moscow, Russia
39: Also at California Institute of Technology, Pasadena, USA
40: Also at Faculty of Physics, University of Belgrade, Belgrade, Serbia
41: Also at Facoltà Ingegneria, Università di Roma, Roma, Italy
42: Also at National Technical University of Athens, Athens, Greece
43: Also at Scuola Normale e Sezione dell'INFN, Pisa, Italy
44: Also at National and Kapodistrian University of Athens, Athens, Greece
45: Also at Warsaw University of Technology, Institute of Electronic Systems, Warsaw, Poland
46: Also at Institute for Theoretical and Experimental Physics, Moscow, Russia
47: Also at Albert Einstein Center for Fundamental Physics, Bern, Switzerland
48: Also at Adiyaman University, Adiyaman, Turkey
49: Also at Mersin University, Mersin, Turkey
50: Also at Cag University, Mersin, Turkey

51: Also at Piri Reis University, Istanbul, Turkey
52: Also at Gaziosmanpasa University, Tokat, Turkey
53: Also at Ozyegin University, Istanbul, Turkey
54: Also at Izmir Institute of Technology, Izmir, Turkey
55: Also at Mimar Sinan University, Istanbul, Istanbul, Turkey
56: Also at Marmara University, Istanbul, Turkey
57: Also at Kafkas University, Kars, Turkey
58: Also at Yildiz Technical University, Istanbul, Turkey
59: Also at Hacettepe University, Ankara, Turkey
60: Also at Rutherford Appleton Laboratory, Didcot, United Kingdom
61: Also at School of Physics and Astronomy, University of Southampton, Southampton, United Kingdom
62: Also at Instituto de Astrofísica de Canarias, La Laguna, Spain
63: Also at Utah Valley University, Orem, USA
64: Also at University of Belgrade, Faculty of Physics and Vinca Institute of Nuclear Sciences, Belgrade, Serbia
65: Also at Argonne National Laboratory, Argonne, USA
66: Also at Erzincan University, Erzincan, Turkey
67: Also at Texas A&M University at Qatar, Doha, Qatar
68: Also at Kyungpook National University, Daegu, Korea